Redundant Filterbank Precoders and Equalizers Part I: Unification and Optimal Designs

Anna Scaglione, *Student Member, IEEE*, Georgios B. Giannakis, *Fellow, IEEE*, and Sergio Barbarossa, *Member, IEEE*

***Abstract*—Transmitter redundancy introduced using filterbank precoders generalizes existing modulations including OFDM, DMT, TDMA, and CDMA schemes encountered with single- and multiuser communications. Sufficient conditions are derived to guarantee that with FIR filterbank precoders FIR channels are equalized perfectly in the absence of noise by FIR zero-forcing equalizer filterbanks, *irrespective* of the channel zero locations. Multicarrier transmissions through frequency-selective channels can thus be recovered even when deep fades are present. Jointly optimal transmitter-receiver filterbank designs are also developed, based on maximum output SNR and minimum mean-square error criteria under zero-forcing and fixed transmitted power constraints. Analytical performance results are presented for the zero-forcing filterbanks and are compared with mean-square error and ideal designs using simulations.**

***Index Terms*— Block transmissions, communications, digital subscriber loops, discrete-multitone and discrete-wavelet multiplexing, downlink channels, filterbanks, intersymbol and interchip interference, joint transceiver optimization, minimum mean-square error receivers, orthogonal frequency-division multiplexing, precoding, pre-equalization, time- and code-division multiple access, zero-forcing.**

I. Introduction

REDUNDANCY at the transmitter builds diversity in the input of digital communication systems and is well motivated for designing error correcting codes (see e.g., [2, ch. 9]). However, especially with block transmissions, where the data stream is divided into consecutive equal-size blocks [11], the redundancy added to each block offers also a powerful tool for removing interblock interference and devising simple yet effective schemes for intersymbol-interference (ISI) suppression. Examples of block transmissions include orthogonal frequency division multiplexing (OFDM) [10], coded-OFDM (COFDM) [41], discrete multitone (DMT) [3], [19], [25], and pseudo-random or wavelet based precoded transmissions for code-division or discrete-wavelet multiple access (CDMA/DWMA) [1], [26], [30], [38]. Recently, input redundancy has also been exploited for blind ISI mitigation [13], [32] to obviate channel zero restrictions imposed by spatio-temporal output diversity methods relying on fractional sampling and/or multiple-antenna reception [22], [33], [34]. As opposed to error correcting coders, block-precoded transmitters operate in the complex field rather than the Galois field and explicitly take into account the presence of frequency-selective fading.

Despite the high potential of block transmission systems, a unifying framework able to encompass existing modulations and equalization schemes, as well as general channel identifiability conditions leading to improved optimal design alternatives, is lacking. As will be discussed in detail in Sections II and III, a good candidate is the multirate filterbank transceiver model, which has also been considered in [1], [10], [13], [30]–[32], and [36]–[39]. Perfect reconstruction (PR) synthesis filterbanks at the transmitter and analysis filterbanks at the receiver allow perfect recovery of communication symbols, but the challenges arise with ISI-inducing channels and noise, both of which destroy the PR property. Filterbank (FB) transceivers for ISI and noise mitigation will be our focus herein. In a different context, PRFB's have been used also as data compressing transforms designed to optimize coding gains and suppress quantization noise (see e.g., [9], [17], and references therein).

Building on the filterbank precoding framework, our objective in this paper is threefold: i) to unify the aforementioned modulation/precoding schemes under the filterbank framework of Fig. 1 (Section III); ii) to develop sufficient conditions for existence of FIR zero-forcing (ZF) filterbanks, which, in the absence of noise, equalize perfectly any FIR channel using FIR decoder filterbanks (Section IV); and iii) to derive jointly optimal FIR transmitter-receiver filterbank pairs, which, in the presence of noise, maximize the output SNR or minimize mean-square error under transmitted power constraints (Section V). Simulations are presented in Section VI and concluding remarks in Section VII.

II. Filterbank Transceiver Model

Fig. 1 shows the discrete-time multirate equivalent model of our baseband communication system using filterbank precoders. The input serial data stream $s(n)$ is converted into M parallel substreams $s_m(n) := s(nM+m)$, where $s_m(n)$ denotes the mth symbol in the nth block of M symbols, distributed on the M filterbank branches via advance-elements and downsamplers by M. Upsamplers by P insert $P-1$ zeros after each symbol, and the mth upsampler's output is $\sum_{i=-\infty}^{\infty} s(iM+m)\delta(n-iP)$, where $\delta(n)$ denotes Kronecker's delta. Assuming $P > M$, the redundancy introduced per

Manuscript received September 8, 1997; revised October 30, 1998. This work was supported by the National Science Foundation under Grant CCR-9805350. Part of the results in this paper were presented at the Allerton Conference, September 1997, and the International Conference on Communications, June 1998. The associate editor coordinating the review of this paper and approving it for publication was Dr. Truong Q. Nguyen.

A. Scaglione and S. Barbarossa are with the Infocom Department, University of Rome "La Sapienza," Roma, Italy (e-mail: sergio@infocom.ing.uniroma1.it; annas@infocom.ing.uniroma1.it).

G. B. Giannakis is with the Department of Electrical and Computer Engineering, University of Minnesota, Minneapolis, MN 55455 USA (e-mail: georgios@ece.umn.edu).

Publisher Item Identifier S 1053-587X(99)04642-5.

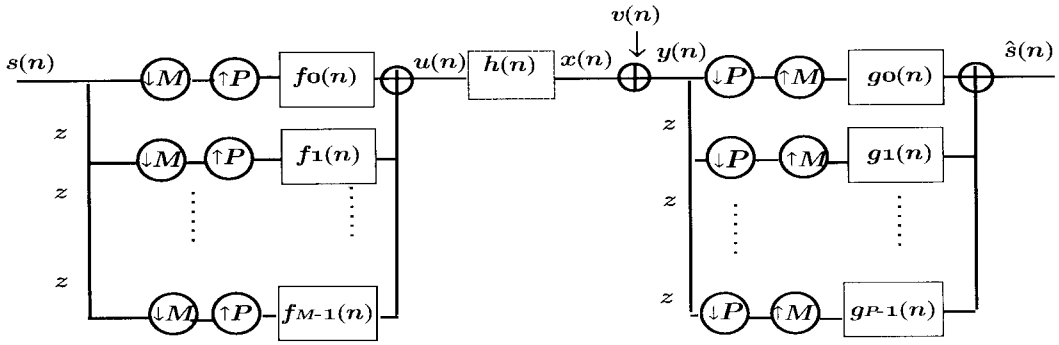

Fig. 1. Multirate discrete-time baseband equivalent transmitter/channel/receiver model.

transmitted block is measured by the ratio $(P-M)/P$, whereas at the receiver, the rate is reduced by the same amount restoring the original input data rate. Indicating by $\{f_m(n)\}_{m=0}^{M-1}$ the impulse responses of filters at each branch of the transmit filterbank, our precoder's output is[1]

$$u(n)=\sum_{m=0}^{M-1}\sum_{i=-\infty}^{\infty} s(iM+m)f_m(n-iP). \tag{1}$$

From an input–output (I/O) point of view, our transmit-filterbank precoder takes size-M blocks of $s(n)$, vector filters them, and maps them to size-P blocks of $u(n)$. After passing through the linear time-invariant (LTI) channel $h(l)$, the data received in additive Gaussian noise (AGN) $v(n)$ are

$$\begin{aligned} y(n)=x(n)+v(n)&=\sum_{l=-\infty}^{\infty} h(l)u(n-l)+v(n)\\ &=\sum_{m=0}^{M-1}\sum_{i=-\infty}^{\infty} s(iM+m)\\ &\quad\cdot\sum_{l=-\infty}^{\infty} h(l)f_m(n-l-iP)+v(n). \end{aligned} \tag{2}$$

A mapping mirror to (1) takes place at the receiver, where size-P blocks of $y(n)$ are mapped to size-M blocks of $\hat{s}(n)$ after being filtered through the receive-filterbank composed, in general, of P branches

$$\hat{s}(n)=\sum_{p=0}^{P-1}\sum_{j=-\infty}^{\infty} y(jP+p)g_p(n-jM). \tag{3}$$

Although (1)–(3) result in a rather cumbersome I/O relationship, they can be expressed compactly in a matrix form. Let $\boldsymbol{s}(n)$ and $\hat{\boldsymbol{s}}(n)$ be the $M\times 1$ polyphase vectors $\boldsymbol{s}(n):=(s(nM), s(nM+1),\cdots, s(nM+M-1))^T$ and $\hat{\boldsymbol{s}}(n):=(\hat{s}(nM), \hat{s}(nM+1),\cdots, \hat{s}(nM+M-1))^T$, respectively. Denote by $\boldsymbol{u}(n)$, $\boldsymbol{y}(n)$ the $P\times 1$ vectors $\boldsymbol{u}(n):=(u(nP), u(nP+1),\cdots, u(nP+P-1))^T$ and $\boldsymbol{y}(n):=(y(nP), y(nP+1),\cdots, y(nP+P-1))^T$, respectively. The vector form of (1) and (3) then becomes

$$\boldsymbol{u}(n)=\sum_{i=-\infty}^{\infty}\boldsymbol{F}_i\boldsymbol{s}(n-i) \tag{4}$$

$$\hat{\boldsymbol{s}}(n)=\sum_{j=-\infty}^{\infty}\boldsymbol{G}_j\boldsymbol{y}(n-j) \tag{5}$$

where the elements of the $P\times M$ and $M\times P$ matrices $\boldsymbol{F}_i$ and $\boldsymbol{G}_j$ are

$$\{\boldsymbol{F}_i\}_{p,m}:=f_m(iP+p),\ \{\boldsymbol{G}_j\}_{m,p},:=g_p(jM+m) \tag{6}$$

$$m=0,\cdots,M-1,\qquad p=0,\cdots,P-1 \tag{7}$$

with the columns of the ith (jth) matrix $\boldsymbol{F}_i$ ($\boldsymbol{G}_j$) containing the ith (jth) segment of length P (M) of the filters' impulse responses $\{f_m(n)\}_{m=0}^{M-1}$ ($\{g_p(n)\}_{p=0}^{P-1}$). The transmit and receive filterbanks in the system of Fig. 1 have the same structure, contrary to what is usually employed in the perfect reconstruction (PR) filterbank literature [35], where filterbanks have equal number of branches but filters, up/downsamplers, and delays are located on the opposite side relative to Fig. 1. However, the two structures can be made equivalent. In fact, (6) and (7) establish that $\{\boldsymbol{F}_i\}_{p,m}=f_m(iP+p)$ and $\{\boldsymbol{G}_j\}_{m,p}=g_p(jM+m)$. Defining P filters $\phi_p(n)$ [M filters $\gamma_m(n)$] such that $\{\boldsymbol{F}_i\}_{p,m}=\phi_p(iM+m)\equiv f_m(iP+p)$ ($\{\boldsymbol{G}_j\}_{m,p}=\gamma_m(jP+p)\equiv g_p(jM+m)$), the I/O relationship remains unchanged. Hence, to preserve the same matrices $\boldsymbol{F}_i$ ($\boldsymbol{G}_j$), the filterbank built with filters $\phi_p(n)$ ($\gamma_m(n)$) must have a number of branches equal the number of rows of $\boldsymbol{F}_i$ ($\boldsymbol{G}_j$), with the P (M) filters $\phi_p(n)$ ($\gamma_m(n)$) in each branch followed by the down-upsamplers and delays. Every property derived on matrices $\boldsymbol{F}_i$ and $\boldsymbol{G}_j$ applies to both structures, but in this paper, we will adopt the one in Fig. 1 and the corresponding matrix notation.

An FIR filterbank has filters $\{f_m(n)\}_{m=0}^{M-1}$ ($\{g_p(n)\}_{p=0}^{P-1}$) that are FIR, which renders the infinite sums in (1) and (3) finite. In order to generalize our matrix formulation to the LTI-channel I/O relationship, let the $P\times 1$ vector $\boldsymbol{x}(n):=(x(nP), x(nP+1),\cdots, x(nP+P-1))^T$ denote the noise-free block of the channel output and $\boldsymbol{v}(n)$ the corresponding

[1]We assume continuous-time Nyquist signaling pulses; hence, their effect disappears in the discrete-time equivalent model [24, pp. 542–547].

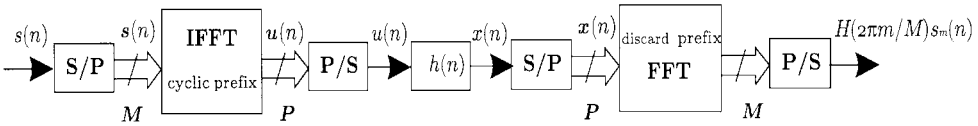

Fig. 2. Conventional OFDM transmitter/channel/receiver model (S/P: serial to parallel).

AGN vector. The received data block is then given by

$$\boldsymbol{y}(n)=\boldsymbol{x}(n)+\boldsymbol{v}(n)=\sum_{l=-\infty}^{\infty}\boldsymbol{H_l}\boldsymbol{u}(n-l)+\boldsymbol{v}(n) \quad (8)$$

where the $P\times P$ matrices $\boldsymbol{H_l}$ are defined as

$$\boldsymbol{H_l}:=\begin{pmatrix} h(lP) & \cdots & h(lP-P+1) \\ \vdots & \ddots & \vdots \\ h(lP+P-1) & \cdots & h(lP) \end{pmatrix}. \quad (9)$$

Based on (4)–(9), we can write

$$\hat{\boldsymbol{s}}(n)=\sum_{j,\,l,\,i=-\infty}^{\infty}\boldsymbol{G}_j\boldsymbol{H_l}\boldsymbol{F}_i\boldsymbol{s}(n-l-i-j)+\sum_{j=-\infty}^{\infty}\boldsymbol{G}_j\boldsymbol{v}(n-j). \quad (10)$$

Using the matrix formulation presented so far, transmit- and receive-filterbanks deal with data blocks (vectors) as LTI filters do over sequences of individual samples. Transmit-redundancy offers degrees of freedom that one can exploit to improve system performance. The general problem of block equalization can also be formulated in the $\mathcal{Z}$-domain using vector (matrix) $\mathcal{Z}$-transforms, rendering (10) a matrix/vector product relationship $\hat{\boldsymbol{\mathcal{S}}}(z)=\boldsymbol{\mathcal{G}}(z)\boldsymbol{\mathcal{H}}(z)\boldsymbol{\mathcal{F}}(z)\boldsymbol{\mathcal{S}}(z)+\boldsymbol{\mathcal{G}}(z)\boldsymbol{\mathcal{V}}(z)$, and relevant conditions for the general case of channel equalization can be found in [30] and [39]. In this paper, we will concentrate on the FIR channel case, and we will explicitly exploit the limited interblock interference to express the conditions on the filterbanks in the time domain. In particular, it will be shown in Section IV that an FIR filterbank at the receiver can equalize exactly an FIR channel (irrespective of its zero locations), provided that $P>M$. The next section highlights the importance of this issue for existing transmission techniques in communication systems that can be interpreted under the filterbank framework discussed so far.

III. Unifying Filterbank Precoders

A number of single and multiuser modulation schemes fall under the filterbank model of Fig. 1. We outline some in this section in order to motivate subsequent results and illustrate their generality.

1) OFDM/DMT: Both are multicarrier techniques with precoding filters

$$f_m(n)=e^{j(2\pi/M)mn}, \qquad m\in[0,\,M-1],\ n\in[0,\,P-1]$$
$$P=M+\overline{L} \quad (11)$$

where $\overline{L}\geq L$ is an upper bound of the FIR channel order L. Because $f_m(n)=0$ for $n\notin[0,\,P-1]$, the only nonvanishing summand (over i) in computing the pth component $u_p(n):=u(nP+p)$ from (1) corresponds to $i=n$; hence, using the definition $s_m(n):=s(nM+m)$, we find

$$u_p(n)=\sum_{m=0}^{M-1}s_m(n)e^{j(2\pi/M)mp}, \qquad p=0,\,1,\,\cdots,\,P-1. \quad (12)$$

For each block (fixed n), (12) amounts to taking the inverse FFT (IFFT) of the M-samples long sequence $\{s_m(n)\}_{m=0}^{M-1}$ (see also Fig. 2). Notice though that P samples of the IFFT are taken, and since $P>M$, we have $P-M=\overline{L}$ samples of $u_p(n)$ that are wrapped around in each block. This portion of $u_p(n)$ is referred to as the cyclic prefix or suffix, depending on whether the redundant $\overline{L}$ samples are appended at the beginning or the end of the block [5] [filters in (11) correspond to a cyclic suffix].

If, in addition to having $f_m(n)$ FIR of order $P-1$, we also select $\overline{L}\geq L$, then for $p=L,\cdots,P-1$, the only nonvanishing summand (over i) in (2) corresponds to $i=n$, and we obtain

$$x_p(n):=x(nP+p)=\sum_{m=0}^{M-1}s_m(n)\sum_{l=0}^{L}h(l)f_m(p-l)$$
$$=\sum_{m=0}^{M-1}s_m(n)e^{j(2\pi/M)mp}H(2\pi m/M) \quad (13)$$

where $H(\omega):=\sum_{l=0}^{L}h(l)\exp(-j\omega l)$ is the channel transfer function. Equation (13) illustrates how multicarrier techniques turn a convolutive (or frequency-selective) channel into a superposition of M multiplicative (flat fading) channels. At the OFDM receiver filterbank, the filters $g_p(n)$ are chosen as

$$g_p(n)=\frac{1}{M}\,e^{-j(2\pi/M)(p+\overline{L})n}\neq 0$$
$$\text{for } p\in[\overline{L},\,P-1] \text{ and } n\in[0,\,M-1]. \quad (14)$$

Note that the $\overline{L}$ leading $g_p(n)$ filters are zero. Because $g_p(n)=0$ for $n\notin[0,\,M-1]$, the only nonvanishing summand (over i) in (3) corresponds to $j=n$; thus, the mth component of the noise-free output is $\hat{s}_m(n):=\hat{s}(nM+m)=\sum_{p=\overline{L}}^{P-1}x_p(n)g_p(m)$. Taking into account (14), the latter corresponds to discarding the first $\overline{L}$ samples $\{x_p(n)\}_{p=0}^{L-1}$ of each block. Taking the FFT of the remaining M samples in each block and using (13) and (14), we arrive at (see also Fig. 2)

$$\zeta_m(n)=\frac{e^{-j(2\pi/M)\overline{L}m}}{M}\sum_{p=\overline{L}}^{P-1}x_p(n)e^{-j(2\pi/M)pm}$$
$$=H\left(\frac{2\pi}{M}\,m\right)s_m(n),$$
$$\hat{s}_m(n)=\zeta_m(n)/H\left(\frac{2\pi}{M}\,m\right). \quad (15)$$

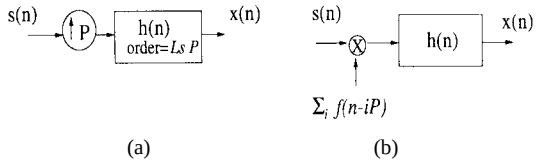

Fig. 3. Discrete-time baseband equivalent models for (a) output fractional sampling and (b) periodically modulated input.

Equation (15) points out the difficulty in equalizing channels with unit circle zeros located at (or close to) angles $2\pi m/M$.

Although this problem is well known to the OFDM community [10], the view of Fig. 2 as a special case of Fig. 1 will prove quite insightful in equalizing channels having zeros on the unit circle. This is very interesting especially for OFDM systems whose popularity originates from the ease with which they handle frequency-selective channels. If unit circle channel zeros are known, the frequencies corresponding to channel nulls are avoided in existing approaches so that (15) can be inverted by transmitting information over the nonfaded frequencies (subchannels). The resulting so-called DMT transmission has been selected by the ANSI-T1E1.4 Committee for ADSL applications [25]. If the channel status is not exactly known at the transmitter side, coded-OFDM (COFDM) is used to recover the errors arising at the faded subchannels at the expense of reduced efficiency. COFDM has been selected as the standard transmultiplexer for digital audio and video broadcasting (DAB-DVB) applications in Europe [5], [8].

With FIR wavelets replacing complex exponentials in (11), potential benefits may arise, as reported in [26] and [38].

2) Fractional Sampling/Periodic Input Modulation: These schemes have one thing in common: They both induce cyclostationarity at the received time series without introducing redundancy at the input. Let us consider fractional sampling by a factor P of the continuous-time data $x_c(t) = \sum_i s(i)h_c(t - iT_s - \epsilon)$, where T_s denotes symbol period and ϵ timing ambiguity. The discrete-time baseband equivalent model in this case is

$$x(n) := x_c(nT_s/P) = \sum_i s(i)\, h(n - iP) \tag{16}$$

where $h(n) := h_c(nT_s/P - \epsilon)$. If the continuous-time channel introduces ISI of L_s symbols, i.e., $h_c(t) = 0$ for $t \notin [0,\, L_sT_s]$, then $h_c(nT_s/P) = 0$ for $nT_s/P \notin [0,\, L_sT_s]$, and the discrete-time channel has $h(n) = 0$ for $n \notin [0,\, L_sP]$. Hence, fractional sampling by a factor P can be described by Fig. 3(a), which can be viewed as a special case of Fig. 1 with $M = 1$, $f_0(n) = \delta(n)$, and $L = L_sP$ (note that here, L_s denotes the symbol rate FIR channel order; see also [15]).

With $c(n)$ denoting a pseudo-random sequence and $f_0(n) = c(n)$, the block diagram in Fig. 3(a) also represents direct-sequence spread-spectrum systems with spreading factor P [31]. A setup with a single user and P receiving antennas as in [14] and [22] is also described by Fig. 1 with $M = 1$ defining $h_p(n) := h(nP + p)$, where $h_p(n)$ denotes the impulse response of the pth channel with $p = 0, \cdots, P-1$, $n = 0, \cdots, L$, and L is the maximum channel order.

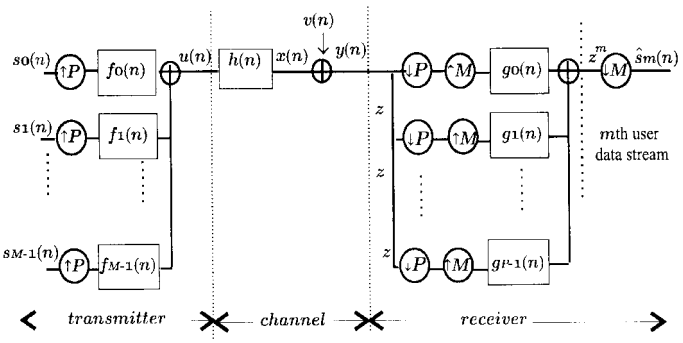

Fig. 4. Multiuser multirate discrete-time model for the downlink.

Input $s(n)$ modulated by a P-periodic sequence $f(n) = f(n + P)$ yields $u(n) = f(n)s(n)$ and has been used in [4] and [29] for blind channel estimation. We wish to show that such sequences can be transmitted also with the precoders of Fig. 1 by choosing $P = M$ and $f_m(n) = f(m)\delta(n - m)$, $m \in [0,\, M-1]$. Indeed, starting with (2) and plugging these precoding filters, we find

$$\begin{aligned} x(n) &= \sum_{i=-\infty}^{\infty} \sum_{m=0}^{P-1} s(iP+m) \sum_{l=0}^{L} h(l)f(m) \\ &\quad \cdot \delta(n-l-iP-m) \\ &= \sum_{l=0}^{L} h(l)s(n-l) \left[\sum_{i=-\infty}^{\infty} f(n-l-iP) \right] \end{aligned} \tag{17}$$

where the term in square brackets denotes the periodic modulating sequence $f(n)$ with period P [see also Fig. 3(b)].

3) (De-)Interleaving:

Especially when combating fading over channels characterized by bursty errors [2], it is known that storing blocks of M data row-wise in an $R \times C$ matrix ($M = RC$) and reading the matrix column-wise yields an output less correlated than the input. Interestingly, such a coding operation is also possible with the filterbank precoder if we select $R \leq C$ and, for $m \in [0,\, M-1]$, $n \in [0,\, P-1]$, choose the filters

$$f_m(n) = \delta(n - (cR + q)), \qquad m = qC + c,\ c \in [0,\, C-1]. \tag{18}$$

Note that while $f_0(n) = \delta(n)$ yields an output $u_0(n) = \{s(0)0 \cdots 0s(M)0 \cdots\}$, the filter $f_C(n) = \delta(n-1)$ yields an output $u_C(n) = \{0s(C)0 \cdots 0s(2C)0 \cdots\}$, i.e., $s(0)$ is followed by $s(C)\ s(2C) \cdots s((R-1)C)$, illustrating the interleaving process.

Deinterleaving is achieved similarly by reversing the roles of $C(c)$ and $R(r)$ in (18) as in

$$g_p(n) = \delta(n - (rC + q)), \qquad p = qR + r,\ r \in [0,\, R-1].$$

4) TDMA/FDMA/CDMA: For these multiuser schemes, no blocking occurs at the precoder, and the receiver filters'

outputs are properly selected (see Fig. 4). In the uplink, the base station receives the signal from each user convolved with a different channel impulse response $\{h_m(l)\}_{l=0}^{L}$. In the downlink, the mth user receives the multiplexed signal convolved with the channel $h_m(l) = h(l)\ \forall m \in [0, M-1]$. The ability of reconstructing the vector of multiplexed data $\boldsymbol{s}(n) := (s_0(n) \cdots s_{M-1}(n))^T$ is a sufficient condition to recover the data stream of, say, user m, by simply selecting the mth component of interest from $\boldsymbol{s}(n)$. The downlink single channel case considered herein applies also when many users are multiplexed for a point-to-point relay, where all users share a common channel (say, from a distant base station to the service provider's central switching office), and in such a case, the overall vector $\boldsymbol{s}(n)$ has to be recovered by the receiver.

For TDMA transmission, the precoder filterbank uses $f_m(n) = \delta(n-m)$ with $P = M + \overline{L}$, where $\overline{L} \geq 0$ is the length of the so-called guard interval ($\overline{L}$ trailing zeros); see also [18]. In FDMA, $f_m(n) = \exp(j2\pi f_m n)$, where f_m is the carrier assigned to the mth user.

In CDMA, $f_m(n) = c_m(n)$, where $c_m(n)$ denotes the m-user's discrete-time equivalent code (at the chip rate), and P is the so-called processing (or spreading) gain (see [30] and [38] for detailed description of the multirate CDMA model and [1] for a recent review).

IV. FIR-ZF Equalizing Filterbanks

With moderate or large number of filters M in the precoder, the maximum likelihood receiver implemented with Viterbi's algorithm has prohibitively large complexity which motivates looking for linear (and preferably low order FIR) equalizing filterbanks. In this section, we will focus on zero-forcing (ZF) solutions because they offer (almost) perfect symbol recovery in (high SNR) noise-free environments, and their performance in terms of error probability is easily computable. Thanks to their reduced complexity, linear equalizers are widely used in practice to (re-)initialize decision feedback equalizers (DFE's) that improve performance by capitalizing on the finite-alphabet of the source. Designs in the presence of noise will be pursued in Section V. Based on (10), our goal in this section is to *identify the conditions on the transmit filters* $\{f_m(n)\}_{m=0}^{M-1}$ *that allow for perfect symbol recovery through an FIR filterbank of order* $Q-1$ $\{\boldsymbol{G}_q\}_{q=0}^{Q-1}$, *irrespective of the FIR channel zero locations*. We will adopt the following assumptions.

- **a0)** Channel $h(l)$ is Lth order FIR with $h(0),\ h(L) \neq 0$.
- **a1)** (P, M, L) are chosen such that the triplet (P, M, L) satisfies: $P > M$ and $P > L$.
- **a2)** Transmit filters $\{f_m(n)\}_{m=0}^{M-1}$ are causal [$f_m(n) = 0$ for $n < 0$] and of length $\leq P$ [$f_m(n) = 0$ for $n \geq P$], and receive filters $\{g_p(n)\}_{p=0}^{P-1}$ are causal and of length QM. In particular, we select matrix $\boldsymbol{F}_0$ in (6) to be full column rank, i.e., rank$(\boldsymbol{F}_0) = M$.

Assumptions a1) and a2) as well as (6) and (7) imply that the transmit filterbank is modeled as $\boldsymbol{F}_i = \boldsymbol{F}_0\delta(i)$ and the receive filterbank as $\boldsymbol{G}_j = \sum_{q=0}^{Q-1} \boldsymbol{G}_q\delta(j-q)$, whereas from assumption a0) and (9), we have that the channel is described by $\boldsymbol{H}_l = \boldsymbol{H}_0\delta(l) + \boldsymbol{H}_1\delta(l-1)$ with

$$\boldsymbol{H}_0 := \begin{pmatrix} h(0) & 0 & 0 & \cdots & 0 \\ \vdots & h(0) & 0 & \cdots & 0 \\ h(L) & \cdots & \ddots & \cdots & \vdots \\ \vdots & \ddots & \cdots & \ddots & 0 \\ 0 & \cdots & h(L) & \cdots & h(0) \end{pmatrix}$$

$$\boldsymbol{H}_1 := \begin{pmatrix} 0 & \cdots & h(L) & \cdots & h(1) \\ \vdots & \ddots & 0 & \ddots & \vdots \\ 0 & \cdots & \ddots & \cdots & h(L) \\ \vdots & \vdots & \vdots & \ddots & \vdots \\ 0 & \cdots & 0 & \cdots & 0 \end{pmatrix}. \tag{19}$$

Because of the finite channel memory and a1), matrix $\boldsymbol{H}_1$ has nonzero elements only in its $L \times L$ top right submatrix, which models the fact that only the first L samples of the nth received block $\boldsymbol{x}(n)$ will be affected by the ISI of the last L samples of the $(n-1)$st transmitted block $\boldsymbol{u}(n-1) = \boldsymbol{F}_0\boldsymbol{s}(n-1)$.

Thanks to a0)–a2), the decoded symbols are [cf. (5)]

$$\hat{\boldsymbol{s}}(n) = \sum_{q=0}^{Q-1} \boldsymbol{G}_q\boldsymbol{x}(n-q) = (\boldsymbol{G}_{Q-1} \cdots \boldsymbol{G}_0)\overline{\boldsymbol{x}}(n) \tag{20}$$

where $\overline{\boldsymbol{x}}^T(n) := (\boldsymbol{x}^T(n-Q+1), \cdots, \boldsymbol{x}^T(n))$, and

$$\begin{aligned} \boldsymbol{x}(n) &= \boldsymbol{H}_0\boldsymbol{u}(n) + \boldsymbol{H}_1\boldsymbol{u}(n-1) \\ &= \boldsymbol{H}_0\boldsymbol{F}_0\boldsymbol{s}(n) + \boldsymbol{H}_1\boldsymbol{F}_0\boldsymbol{s}(n-1). \end{aligned} \tag{21}$$

From (20) and (21), we infer that $\boldsymbol{s}(n-Q)$ is the most remote transmitted block affecting not only the current block $\hat{\boldsymbol{s}}(n)$ but the previous block $\hat{\boldsymbol{s}}(n-1)$ as well. Due to the structure of $\boldsymbol{H}_1$ in (19), interblock interference (IBI) from $\boldsymbol{s}(n-Q)$ is cancelled if and only if $\boldsymbol{G}_{Q-1}\boldsymbol{H}_1\boldsymbol{F}_0 = \boldsymbol{0}_{M\times M}$. For this to hold, it suffices to choose the rows of $\boldsymbol{G}_{Q-1}$ in the left null space $\mathcal{N}(\boldsymbol{H}_1)$. However, from (19), we infer that $\mathcal{N}(\boldsymbol{H}_1)$ is spanned by the canonical vectors $\boldsymbol{1}_i := (0 \cdots 1_{i\text{th-entry}} \cdots 0)^T$ for $i = L+1, \cdots, P$. Hence, in order to eliminate IBI, it suffices to choose

$$\boldsymbol{G}_{Q-1} = (\boldsymbol{0}_{M\times L}\tilde{\boldsymbol{G}}_{Q-1}) \tag{22}$$

which clearly implies $\boldsymbol{G}_{Q-1}\boldsymbol{H}_1 = \boldsymbol{0}$. Unless the precoder matrix is specially designed, condition $\boldsymbol{G}_{Q-1}\boldsymbol{H}_1 = \boldsymbol{0}$ is also necessary if $\boldsymbol{G}_{Q-1}\boldsymbol{H}_1\boldsymbol{F}_0 = \boldsymbol{0}$ is to hold for any $\boldsymbol{F}_0$ satisfying a2).

In summary, IBI is cancelled $\forall\ \boldsymbol{F}_0$ satisfying a2) under the equivalent conditions

$$\begin{aligned} \boldsymbol{G}_{Q-1}\boldsymbol{H}_1\boldsymbol{F}_0 = \boldsymbol{0}_{M\times M} &\Leftrightarrow \boldsymbol{G}_{Q-1}\boldsymbol{H}_1 = \boldsymbol{0}_{M\times M} \\ &\Leftrightarrow \boldsymbol{G}_{Q-1} = (\boldsymbol{0}_{M\times L}\tilde{\boldsymbol{G}}_{Q-1}). \end{aligned} \tag{23}$$

To capture the channel-equalizer effect in a matrix form, we define the $(QP-L)\times QP$ Sylvester matrix

$$\boldsymbol{\mathcal{H}} := \begin{pmatrix} h(L) & \cdots & h(0) & \cdots & 0 \\ \vdots & \ddots & \vdots & \ddots & \vdots \\ 0 & \cdots & h(L) & \cdots & h(0) \end{pmatrix} \tag{24}$$

the *extended* $QP \times QM$ precoder matrix $\boldsymbol{\mathcal{F}}$, and the $M \times (QP - L)$ equalizer matrix:

$$\boldsymbol{\mathcal{F}} := (\boldsymbol{I}_{Q\times Q} \otimes \boldsymbol{F}_0), \qquad \boldsymbol{\mathcal{G}} := (\tilde{\boldsymbol{G}}_{Q-1} \cdots \boldsymbol{G}_0) \tag{25}$$

where $\otimes$ stands for the Kronecker product, and $\boldsymbol{I}_{Q\times Q}$ denotes the $Q \times Q$ identity matrix. We will call P-periodic precoding the case where $\boldsymbol{F}_0$ is constant for every block $q = 1, \cdots, Q$, as opposed to the aperiodic precoding, corresponding to the case where the extended precoder is a block diagonal matrix

$$\boldsymbol{\mathcal{F}} = \text{diag}\Big(\boldsymbol{F}_0^{(1)}, \cdots, \boldsymbol{F}_0^{(Q)}\Big). \tag{26}$$

We also introduce the *extended* $QP \times 1$ and $QM \times 1$ data blocks as

$$\begin{aligned} \overline{\boldsymbol{u}}^T(n) &:= \big(\boldsymbol{u}^T(n-Q+1), \cdots, \boldsymbol{u}^T(n)\big) \\ \overline{\boldsymbol{s}}^T(n) &:= \big(\boldsymbol{s}^T(n-Q+1), \cdots, \boldsymbol{s}^T(n)\big) \end{aligned} \tag{27}$$

and using (20), we obtain the I/O relationship

$$\hat{\boldsymbol{s}}(n) = \boldsymbol{\mathcal{G}}\boldsymbol{\mathcal{H}}\overline{\boldsymbol{u}}(n) = \boldsymbol{\mathcal{G}}\boldsymbol{\mathcal{H}}\boldsymbol{\mathcal{F}}\overline{\boldsymbol{s}}(n) \tag{28}$$

where, in deriving the second equality, we used $\boldsymbol{u}(n) = \boldsymbol{F}_0\boldsymbol{s}(n)$.

From (28), the zero-forcing (ZF), or perfect reconstruction (PR), condition[2] $\hat{\boldsymbol{s}}(n) = \boldsymbol{s}(n)$ is equivalent to

$$\boldsymbol{\mathcal{G}}\boldsymbol{\mathcal{H}}\boldsymbol{\mathcal{F}} = (\boldsymbol{0}_{M\times(Q-1)M}\boldsymbol{I}_{M\times M}). \tag{29}$$

Given $\boldsymbol{\mathcal{H}}$ and $\boldsymbol{\mathcal{F}}$, $\boldsymbol{\mathcal{G}}$ exists if and only if it is possible to invert $\boldsymbol{\mathcal{H}}\boldsymbol{\mathcal{F}}$. Invertibility of the $(QP-L)\times QM$ matrix $\boldsymbol{\mathcal{H}}\boldsymbol{\mathcal{F}}$ requires it to be tall and of full column rank, i.e., for the existence of an FIR-ZF equalizing filterbank, we must have i) $QP - L \geq QM$ and ii) rank$(\boldsymbol{\mathcal{H}}\boldsymbol{\mathcal{F}}) = QM$. To satisfy i), we need to adopt the following.

a1.1) For a given L, select the triplet (P, M, Q) to satisfy a1) as well as $P \geq M + \lceil L/Q \rceil$, with $\lceil\ \rceil$ denoting the ceiling-integer.

When choosing (P, M, Q) to satisfy a1.1), an upper bound $\overline{L} \geq L$ (rather than exact knowledge) of the channel order is all that is required. Given the transmission block size P and the channel order L, a1.1) is met easily by selecting appropriately M and/or the matrix equalizer length Q. Minimum block size P requires $P = M + 1$, and a1.1) is then satisfied with an equalizer of length $Q \geq L$. On the other hand, simple zero-order $(Q = 1)$ receiver filterbanks satisfy a1.1) at the expense of extra redundancy: $P = M + L$ when M is fixed or with extra latency if both P and M have to increase in order to maintain fixed information rate.

With $\mathcal{R}(\mathcal{N})$ denoting range (null) space, the rank condition ii) is satisfied if and only if

$$\mathcal{N}(\boldsymbol{\mathcal{H}}) \bigcap \mathcal{R}(\boldsymbol{\mathcal{F}}) = \{\boldsymbol{0}\} \tag{30}$$

where $\bigcap$ denotes set intersection, and $\{\boldsymbol{0}\}$ is the set containing as unique element the null vector. To explore conditions and precoders $\boldsymbol{\mathcal{F}}$ satisfying (30) irrespective of the channel, we pursue first a characterization of $\mathcal{N}(\boldsymbol{\mathcal{H}})$. Because of a0), the Sylvester matrix $\boldsymbol{\mathcal{H}}$ in (24) has full row rank, implying that the dimensionality of $\mathcal{N}(\boldsymbol{\mathcal{H}})$ is L. Let $\{\rho_l\}_{l=1}^{L}$ denote the channel roots $H(\rho_l) = 0$, and for each root, define the $P \times 1$ Vandermonde vector $\boldsymbol{v}_{l,H} := (1, \rho_l, \cdots, \rho_l^{P-1})^T$ and its augmented $QP \times 1$ counterpart $\overline{\boldsymbol{v}}_{l,H} := (1, \rho_l, \cdots, \rho_l^{QP-1})^T = (1, \rho_l^P, \cdots, \rho_l^{(Q-1)P})^T \otimes \boldsymbol{v}_{l,H}$. It follows by direct substitution that $\boldsymbol{\mathcal{H}}\overline{\boldsymbol{v}}_{l,H} = \boldsymbol{0}$, and thus, $\overline{\boldsymbol{v}}_{l,H} \in \mathcal{N}(\boldsymbol{\mathcal{H}})$ for $l = 1, \cdots, L$. Hence, the set of L linearly independent Vandermonde vectors[3] $\{\overline{\boldsymbol{v}}_{l,H}\colon H(\rho_l) = 0,\ l = 1, \cdots, L\}$ forms a basis for $\mathcal{N}(\boldsymbol{\mathcal{H}})$, i.e., $\mathcal{N}(\boldsymbol{\mathcal{H}}) \equiv \overline{\boldsymbol{\mathcal{V}}}_{L,H} := \text{Span}\{\overline{\boldsymbol{v}}_{l,H}\colon H(\rho_l) = 0,\ l = 1, \cdots, L\}$. Let us define

$$\begin{aligned} \overline{\boldsymbol{\mathcal{V}}}_L := \text{Span}\Big\{ \overline{\boldsymbol{v}}_l,\ \overline{\boldsymbol{v}}_l := \Big(1, v_l, \cdots, v_l^{QP-1}\Big)^T \\ v_l \in \mathbf{C},\ v_{l_1} \neq v_{l_2}\ \forall l_1 \neq l_2,\ l \in [1, L] \Big\} \end{aligned}$$

where $\mathbf{C}$ is the complex field. Note that $\overline{\boldsymbol{\mathcal{V}}}_L$ contains all possible collections of L linearly independent (generalized) Vandermonde vectors and, thus, includes those corresponding to roots of any Lth-order FIR channel. Therefore, to guarantee that (30) holds true *irrespective* of the channel zero locations, denoting by $\overline{\boldsymbol{\mathcal{V}}}_L \equiv \bigcup_{\boldsymbol{h}\in\mathbf{C}^{L+1}} \mathcal{N}(\boldsymbol{\mathcal{H}})$, it is necessary and sufficient that

$$\mathcal{R}(\boldsymbol{\mathcal{F}}) \bigcap \overline{\boldsymbol{\mathcal{V}}}_L = \{\boldsymbol{0}\}. \tag{31}$$

To gain insight about (31), it is worthwhile to enlighten the structure of $\mathcal{R}(\boldsymbol{\mathcal{F}})$. In force of a1), $\boldsymbol{F}_0^{(q)}$ is, in general, a tall matrix and, assuming w.l.o.g. that its first M rows are linearly independent, its last $P - M$ rows can be expressed as a linear combination of the first M rows, allowing for the decomposition

$$\boldsymbol{F}_0^{(q)} = \begin{pmatrix} \boldsymbol{F}^{(q)} \\ \boldsymbol{\Phi}_q\boldsymbol{F}^{(q)} \end{pmatrix} = \begin{pmatrix} \boldsymbol{I} \\ \boldsymbol{\Phi}_q \end{pmatrix}\boldsymbol{F}^{(q)}, \qquad q = 1, \cdots, Q \tag{32}$$

where $\boldsymbol{F}^{(q)}$ is an $M \times M$ full-rank matrix, and $\boldsymbol{\Phi}_q$ is what we could term the *prefix*-generating $(P - M) \times M$ matrix. Then, using (32), we have

$$\begin{aligned} \boldsymbol{\mathcal{F}} &= \text{diag}\Big(\boldsymbol{F}_0^{(1)}, \cdots, \boldsymbol{F}_0^{(Q)}\Big) \\ &= \text{diag}\Big(\big(\boldsymbol{I}\boldsymbol{\Phi}_1^T\big)^T, \cdots, \big(\boldsymbol{I}\boldsymbol{\Phi}_Q^T\big)^T\Big)\text{diag}\Big(\boldsymbol{F}^{(1)}, \cdots, \boldsymbol{F}^{(Q)}\Big) \\ &\Rightarrow \mathcal{R}(\boldsymbol{\mathcal{F}}) = \mathcal{R}\Big[\text{diag}\Big(\big(\boldsymbol{I}\boldsymbol{\Phi}_1^T\big)^T, \cdots, \big(\boldsymbol{I}\boldsymbol{\Phi}_Q^T\big)^T\Big)\Big] \end{aligned} \tag{33}$$

where the last equality holds true because diag$(\boldsymbol{F}^{(1)}, \cdots, \boldsymbol{F}^{(Q)})$ is square and full rank, as per a1).

Therefore, the necessary and sufficient condition for ZF equalization, irrespective of the channnel zeros (31), becomes

$$\mathcal{R}\Big(\text{diag}\Big(\big(\boldsymbol{I}\boldsymbol{\Phi}_1^T\big)^T, \cdots, \big(\boldsymbol{I}\boldsymbol{\Phi}_Q^T\big)^T\Big)\Big) \bigcap \overline{\boldsymbol{\mathcal{V}}}_L = \{\boldsymbol{0}\}. \tag{34}$$

Condition (34) will turn out to be instrumental in establishing our first basic result.

[2] In general, the PR condition can be written as $\hat{\boldsymbol{s}}(n) = \overline{\boldsymbol{s}}(n - d)$, where d denotes a delay that affects equalization performance in the presence of noise. Because d does not affect existence and uniqueness of linear ZF equalizers, w.l.o.g., we take here $d = 0$.

[3] We can always find L such vectors, provided that ρ_l's are distinct. For multiple channel roots, the generalized Vandermonde vectors have to be considered (see e.g., [21]).

Theorem 1—Existence and Uniqueness: Under a0) and a2), the following hold.

1.1) With $P-M<L$ in a1), and

1.1a) using P-periodic precoding, i.e., $\boldsymbol{F}_0^{(q)}=\boldsymbol{F}_0\ \forall q=1,\cdots,Q$ and $\boldsymbol{\mathcal{F}}$ as in (25), the ZF equalizer $\boldsymbol{\mathcal{G}}$ does not exist, irrespective of $\boldsymbol{F}_0$, if the channel has at least one set of $L(\rho)\leq L$ roots v_l lying on a circle of radius ρ at angles that are multiples of $2\pi/P$, i.e., $v_l=\rho\exp(j2\pi k_l/P)$ with k_l integer, $l=1,\cdots,L(\rho)$ and such that $P-M<L(\rho)$;

1.1b) using P-periodic precoding for a given $\boldsymbol{F}_0$ and $\boldsymbol{\Phi}$ if all the L channel roots are also roots of the polynomials formed by the rows of $(\boldsymbol{\Phi},\ -\boldsymbol{I}_{P-M})$, linear FIR ZF equalizers do not exist;

1.1c) selecting Q to satisfy $Q(P-M)\geq P$, there exists an aperiodic precoder, as in (26), that guarantees existence of FIR ZF filterbank equalizers, *irrespective* of the channel zero locations.

1.2) For any (P,M,L), all P-periodic precoders with a cyclic prefix and, in particular OFDM, do not admit a ZF equalizer for channels with one or more zeros located at $v_l=\exp(j2\pi k_l/M)$, with k_l integer.

1.3) With $P-M\geq L$ in a1), the necessary and sufficient condition for the existence of a ZF equalizer for any FIR channel is

a3) $\mathcal{R}(\boldsymbol{F}_0)\bigcap\boldsymbol{\mathcal{V}}_L=\{\boldsymbol{0}\}$, $\forall\ \boldsymbol{\mathcal{V}}_L:=\{(1,v_l,\cdots,v_l^{P-1})^T,\ v_{l_1}\neq v_{l_2}\ \forall\ l_1\neq l_2,\ l,\in[1,L]\}$.

Proof: Consider a vector $\overline{\boldsymbol{\psi}}\in\mathcal{R}(\mathrm{diag}((\boldsymbol{I}\boldsymbol{\Phi}_1^T)^T,\ \cdots,\ (\boldsymbol{I}\boldsymbol{\Phi}_Q^T)^T))$ composed of Q blocks of length P, each of the form $(\boldsymbol{\psi}_q^T,\ \boldsymbol{\psi}_q^T\boldsymbol{\Phi}_q^T)$, $q=1,\cdots,Q$, where $\boldsymbol{\psi}_q$ is an $M\times 1$ vector, and $\boldsymbol{\Phi}_q\boldsymbol{\psi}_q$ is the corresponding $(P-M)\times 1$ prefix, i.e., $\overline{\boldsymbol{\psi}}^T:=[(\boldsymbol{\psi}_1^T,\ \boldsymbol{\psi}_1^T\boldsymbol{\Phi}_1^T),\cdots,(\boldsymbol{\psi}_Q^T,\ \boldsymbol{\psi}_Q^T\boldsymbol{\Phi}_Q^T)]$. With $\overline{\boldsymbol{\nu}}\in\overline{\boldsymbol{\mathcal{V}}}_L$, (34) states equivalently that $\forall(\overline{\boldsymbol{\nu}},\ \overline{\boldsymbol{\psi}})\neq\boldsymbol{0}\not\exists\ \overline{\boldsymbol{\nu}}=\overline{\boldsymbol{\psi}}$. The structure of $\overline{\boldsymbol{\nu}}$ and $\overline{\boldsymbol{\psi}}$ will play a key role in our proof.

1.1a) Using P-periodic coding $\boldsymbol{F}_0^{(q)}=\boldsymbol{F}_0$, and thus $\boldsymbol{\Phi}_q=\boldsymbol{\Phi}$ so that $\mathrm{diag}((\boldsymbol{I}\boldsymbol{\Phi}_1^T)^T,\cdots,(\boldsymbol{I}\boldsymbol{\Phi}_Q^T)^T)=(\boldsymbol{I}_{Q\times Q}\otimes(\boldsymbol{I},\boldsymbol{\Phi}^T)^T)$. Similar to $\overline{\boldsymbol{\psi}}$, decomposing $\overline{\boldsymbol{\nu}}$ in blocks of length P as $(\boldsymbol{\nu}_q^T,\ \boldsymbol{\nu}_q'^T)^T$, where $\boldsymbol{\nu}_q$ is $M\times 1$ and $\boldsymbol{\nu}_q'$ is $(P-M)\times 1$, $\overline{\boldsymbol{\nu}}=\overline{\boldsymbol{\psi}}$ necessarily implies

$$\boldsymbol{\psi}_q=\boldsymbol{\nu}_q\quad\text{and}\quad\boldsymbol{\Phi}\boldsymbol{\psi}_q=\boldsymbol{\nu}_q'\Longleftrightarrow\boldsymbol{\Phi}\boldsymbol{\nu}_q=\boldsymbol{\nu}_q'. \tag{35}$$

Recalling that $\overline{\boldsymbol{\nu}}$ is generated by L Vandermonde vectors as $\overline{\boldsymbol{\nu}}=\sum_{l=1}^{L}\alpha_l\overline{\boldsymbol{v_l}}$ and exploiting the structure of $\overline{\boldsymbol{v_l}}$, we can write $\boldsymbol{\Phi}\boldsymbol{\nu}_q=\boldsymbol{\nu}_q'$ in the explicit form

$$\sum_{l=1}^{L}\alpha_l v_l^{(q-1)P}\boldsymbol{\Phi}(1,\ v_l,\ \cdots,\ v_l^{M-1})^T=\sum_{l=1}^{L}\alpha_l v_l^{(q-1)P}(v_l^M,\ \cdots,\ v_l^{P-1})^T. \tag{36}$$

Defining vector $\boldsymbol{\alpha}=(\alpha_1,\cdots,\alpha_L)^T$ and matrices $\boldsymbol{V}_M,\boldsymbol{V}_{P-M}$ whose columns are, respectively, vectors $(1,v_l,\cdots,v_l^{M-1})^T$ and $(v_l^M,\cdots,v_l^{P-1})^T$, for $l=1,\cdots,L$, (36) becomes

$$[\boldsymbol{\Phi}\boldsymbol{V}_M-\boldsymbol{V}_{P-M}]\,\mathrm{diag}\Big(\Big[v_1^{(q-1)P},\ \cdots,\ v_L^{(q-1)P}\Big]\Big)\boldsymbol{\alpha}=\boldsymbol{0}. \tag{37}$$

To satisfy (37), $\boldsymbol{\alpha}$ should lie in the null space $\mathcal{N}([\boldsymbol{\Phi}\boldsymbol{V}_M-\boldsymbol{V}_{P-M}]\ \mathrm{diag}([v_1^{(q-1)P},\cdots,v_L^{(q-1)P}])$ for $q=1,\cdots,Q$. Condition a1.1) implies $QP-L\geq QM$, and thus, $Q(P-M)\geq L$. Therefore, the number of equations expressed by (37) is greater than or equal to the number of unknowns in $\boldsymbol{\alpha}$. To have a nonzero solution, the equations should be dependent because of the specific structure of $\boldsymbol{\Phi}$ and/or the channel roots v_l, $l=1,\cdots,L$. In particular, if there are $L(\rho)$ channel roots such that $v_l=\rho\exp(j2\pi k_l/P)$, with k_l integer, then there are $L(\rho)$ elements of $\mathrm{diag}([v_1^{(q-1)P},\cdots,v_L^{(q-1)P}])$ that are equal to each other, and $v_l^{(q-1)P}=\rho^{(q-1)P}$, independent of l. Consider w.l.o.g. that these roots define the first $L(\rho)$ Vandermonde vectors $\overline{\boldsymbol{v}}_l$. If $P-M<L(\rho)\leq L$, the $(P-M)\times L(\rho)$ submatrix of $[\boldsymbol{\Phi}\boldsymbol{V}_M-\boldsymbol{V}_{P-M}]$, formed by its first $L(\rho)$ columns, is fat and, thus, rank deficient, independent of $\boldsymbol{\Phi}$. Therefore, there is a nontrivial solution of (37) of the form $\boldsymbol{\alpha}=(\alpha_1,\ \cdots,\ \alpha_{L(\rho)},\ 0,\cdots,0)^T$ that satisfies (37) for every q because

$$\begin{aligned}[\boldsymbol{\Phi}\boldsymbol{V}_M-\boldsymbol{V}_{P-M}]\mathrm{diag}(&[\underbrace{\rho^{(q-1)P},\cdots,\rho^{(q-1)P}}_{L(\rho)},\cdots,v_L^{(q-1)P}])\\&\cdot(\alpha_1,\cdots,\alpha_{L(\rho)},0,\cdots,0)^T\\&=\rho^{(q-1)P}[\boldsymbol{\Phi}\boldsymbol{V}_M-\boldsymbol{V}_{P-M}]\boldsymbol{\alpha}=\boldsymbol{0}.\end{aligned} \tag{38}$$

If $P-M<L$ for P-periodic precoding, the intersection of $\overline{\boldsymbol{\mathcal{V}}}$ with $\mathcal{R}(\boldsymbol{\mathcal{F}})$ contains the vectors $\overline{\boldsymbol{\nu}}=\overline{\boldsymbol{\psi}}=\sum_{l=1}^{L(\rho)}\alpha_l\overline{\boldsymbol{v}}_l\neq\boldsymbol{0}$ with $v_l=\rho\exp(j2\pi k_l/P)$, $l=1,\cdots,L(\rho)$, and $L\geq L(\rho)>P-M$. This contradicts (31) and thus establishes statement 1.1a of the theorem.

1.1b) Denoting by $\boldsymbol{V}_P^T:=(\boldsymbol{V}_M^T,\boldsymbol{V}_{P-M}^T)$ the matrix of the L Vandermonde vectors of length P, (37) is equivalent to

$$[\boldsymbol{\Phi},\ -\boldsymbol{I}_{P-M}]\boldsymbol{V}_P\mathrm{diag}(\boldsymbol{\alpha})\Big(v_1^{(q-1)P},\cdots,v_L^{(q-1)P}\Big)^T=\boldsymbol{0}. \tag{39}$$

If the L channel roots are also roots of the rows of $[\boldsymbol{\Phi},\ -\boldsymbol{I}_{P-M}]$, then $[\boldsymbol{\Phi},\ -\boldsymbol{I}_{P-M}]\boldsymbol{V}_P=\boldsymbol{0}$, and this renders (39) valid $\forall\,\alpha$, proving the statement 1.1b.

1.1c) From (33) and also using (39) with different $\boldsymbol{\Phi}_q$'s, we obtain the counterpart of (37)

$$[\boldsymbol{\Phi}_q,\ -\boldsymbol{I}_{P-M}]\boldsymbol{V}_P\,\mathrm{diag}(\boldsymbol{\alpha})\Big(v_1^{(q-1)P},\cdots,v_L^{(q-1)P}\Big)^T=\boldsymbol{0},\qquad q=1,\cdots,Q. \tag{40}$$

Introducing the $Q(P-M)\times P$ matrix $\boldsymbol{\Psi}^T:=[(\boldsymbol{\Phi}_1,\ -\boldsymbol{I}_{P-M})^T,\ \cdots,\ (\boldsymbol{\Phi}_Q,\ -\boldsymbol{I}_{P-M})^T]$ and stacking (40) for $q=1,\cdots,Q$, we can write

$$\boldsymbol{\Psi}\boldsymbol{V}_P\,\mathrm{diag}(\boldsymbol{\alpha})\begin{pmatrix}1&v_1^P&\cdots&v_1^{(Q-1)P}\\ \vdots&\vdots&\cdots&\vdots\\ 1&v_L^P&\cdots&v_L^{(Q-1)P}\end{pmatrix}=\boldsymbol{0}. \tag{41}$$

If $\boldsymbol{\Psi}\boldsymbol{V}_P$ is full column rank, then there is no possibility to satisfy (41), except for the trivial solution $\boldsymbol{\alpha}=\boldsymbol{0}$. Hence, a sufficient condition for an aperiodic filterbank modulation to guarantee existence of the PR filterbank equalizer $\boldsymbol{\mathcal{G}}$, irrespective of the channel zero locations, is to select precoders with $\boldsymbol{\Phi}_q$'s such that $\mathrm{rank}(\boldsymbol{\Psi})=P$. The latter can be assured by selecting Q such that $Q(P-M)\geq P$ and building $\boldsymbol{\Psi}$ with

at least P independent columns. This requirement can be met by choosing the matrix $(\mathbf{\Phi}_1^T, \cdots, \mathbf{\Phi}_Q^T)^T$, whose M columns must be independent of each other as well as independent of the columns of $(\boldsymbol{I}_{P-M}, \cdots, \boldsymbol{I}_{P-M})^T$. In such a case, the right null-space of Ψ contains only the null vector, and thus, (41) is impossible for any $\boldsymbol{\alpha} \neq \mathbf{0}$; hence, we have not only proved statement 1.1c but also provided a means of constructing aperiodic precoders that guarantee channel-irrespective FIR equalization.

1.2) Systems using a cyclic prefix (e.g., OFDM) are characterized by $\mathbf{\Phi} = (\boldsymbol{I}_{(P-M)\times(P-M)})$.

In general, the matrix $[\mathbf{\Phi}\boldsymbol{V}_M - \boldsymbol{V}_{P-M}]\,\mathrm{diag}([v_1^{(q-1)P}, \cdots, v_L^{(q-1)P}])$ has dimensionality $(P-M)\times L$ and, *if* $P-M<L$, matrix $[\mathbf{\Phi}\boldsymbol{V}_M - \boldsymbol{V}_{P-M}]$ is not full column rank. However, $[\mathbf{\Phi}\boldsymbol{V}_M - \boldsymbol{V}_{P-M}]$ may loose rank even for $P-M \geq L$. In fact, if the channel has at least one zero at $v_l = \exp(j2\pi m_l/M)$, with m_l integer, then the lth column of $[\mathbf{\Phi}\boldsymbol{V}_M - \boldsymbol{V}_{P-M}]$ vanishes because

$$\begin{aligned}\mathbf{\Phi}\left(1, v_l, \cdots, v_l^{M-1}\right)^T &= \left(1, \cdots, e^{j2\pi m_l(P-M-1/M)}\right)^T \\ &\equiv \left(e^{j2\pi(m_l M/M)}, \cdots, e^{j2\pi((m_l(P-1)/M))}\right)^T \\ &= \left(v_l^M, \cdots, v_l^{P-1}\right)^T. \end{aligned} \tag{42}$$

Therefore, $\boldsymbol{\alpha} = (0, \cdots, 0, \alpha_l, 0, \cdots, 0)^T$ with any $\alpha_l \neq 0$ will satisfy (37), and the simple structure of $\boldsymbol{\alpha}$ makes (37) true $\forall\, q$. This proves statement 1.2 of our theorem.

1.3) If a0) and a2) hold and a1) is satisfied with $P = M+L$, then $Q = 1$ is sufficient, and $\boldsymbol{\mathcal{G}} \equiv \boldsymbol{G}_0 = (\boldsymbol{\mathcal{H}}\boldsymbol{F}_0)^\dagger$ if and only if $\mathrm{rank}(\boldsymbol{\mathcal{H}}\boldsymbol{F}_0) \geq M$. Assumption a3) corresponds to the necessary and sufficient condition (31) for $Q = 1$ and guarantees that $rank(\boldsymbol{\mathcal{H}}\boldsymbol{F}_0) \geq M$, $\forall\, \boldsymbol{h}$. Since the structure of $\boldsymbol{F}_0$ is arbitrary, we can build it in order to guarantee a3). For one such constructive algorithm, see Theorem 2. ■

In words, a3) requires $\boldsymbol{F}_0$ to be designed so that linear combinations of its columns are not expressible as linear combinations of L (or less) Vandermonde vectors. Such an interpretation suggests also a systematic algorithm for constructing precoders that satisfy a3) when $P - M \geq L$:

Step 1: Select $M(L+1)$ distinct points $\{v_{m,l}\}$, $m \in [0, M-1]$, $l \in [1, L+1]$ on the complex plane, and corresponding to each point, build a $P\times 1$ Vandermonde vector $\boldsymbol{v}_{m,l} := (1, v_{m,l}, \cdots, v_{m,l}^{P-1})^T$.

Step 2: For each of the M possible sets of $L+1$ Vandermonde vectors, construct the corresponding precoding filter (mth column of $\boldsymbol{F}_0$) as $\boldsymbol{f}_m = \sum_{l=1}^{L+1} \boldsymbol{v}_{m,l}$, $m = 0, 1, \cdots, M-1$; instead of the sum used here, any linear combination with nonzero coefficients would work as well.

Step 3: With the columns constructed as in Step 2, form the precoder matrix $\boldsymbol{F}_0 := (\boldsymbol{f}_0 \;\; \boldsymbol{f}_1 \;\; \cdots \;\; \boldsymbol{f}_{M-1})$, which can be readily shown to satisfy a3).

For $P - M \geq L$, a general class of precoders fulfilling a3) results if we choose the columns $\{f_m(n)\}_{m=0}^{M-1}$ of $\boldsymbol{F}_0$ from the M-dimensional subspace spanned by the P-dimensional canonical basis. Because $P > L$, each of the canonical vectors is given as a linear combination of exactly P Vandermonde vectors, and hence, a3) is satisfied. As we will see in Theorem 2, precoders with trailing zeros offer a special case, but a3) is also satisfied if the L zeros are inserted in arbitrary positions of the filters $f_m(n)$.

Theorem 2—Trailing Precoder Zeros: Suppose that a0) holds, a1) is satisfied with $P = M + L$, and transmitter matrix $\boldsymbol{F}_0$ has trailing zeros [and, thus, a3) holds] and also obeys a2), i.e., $\boldsymbol{F}_0$ assumes the form

$$\boldsymbol{F}_0 = \begin{pmatrix} \boldsymbol{F}_{M\times M} \\ \mathbf{0}_{L\times M} \end{pmatrix} \tag{43}$$

and $\mathrm{rank}(\boldsymbol{F}) = M$. Then, for a given $\boldsymbol{F}$ and channel matrix $\boldsymbol{H}_0$, there exists a zero-order $(Q=1)$ ZF equalizer filterbank so that $\boldsymbol{G}\boldsymbol{x}(n) = \boldsymbol{s}(n)$. With $\boldsymbol{H}$ denoting the first M columns of $\boldsymbol{H}_0$, the minimum norm ZF filterbank is unique and is given by

$$\boldsymbol{G} = (\boldsymbol{H}_0\boldsymbol{F}_0)^\dagger = \boldsymbol{F}^{-1}\boldsymbol{H}^\dagger. \tag{44}$$

Proof: From the definition of $\boldsymbol{H}_1$ in (19), if $\boldsymbol{F}_0$ is selected as in (43), the guard time of L trailing zeros avoids interblock interference, i.e., $\boldsymbol{H}_1\boldsymbol{F}_0 = \mathbf{0}$, and hence

$$\boldsymbol{x}(n) = \boldsymbol{H}_0\boldsymbol{F}_0\boldsymbol{s}(n) = \boldsymbol{H}\boldsymbol{F}\boldsymbol{s}(n). \tag{45}$$

Because $\boldsymbol{H}\boldsymbol{F}$ is a tall matrix, we have

$$\boldsymbol{s}(n) = (\boldsymbol{H}\boldsymbol{F})^\dagger\boldsymbol{x}(n) \tag{46}$$

where $(\boldsymbol{H}\boldsymbol{F})^\dagger$ also gives the minimum norm solution of the linear system of equations $\boldsymbol{G}_0\boldsymbol{x}(n) = \boldsymbol{s}(n)$. Therefore, the minimum norm ZF filterbank is

$$\boldsymbol{G} = (\boldsymbol{H}_0\boldsymbol{F}_0)^\dagger = (\boldsymbol{H}\boldsymbol{F})^\dagger = (\boldsymbol{F}^H\boldsymbol{H}^H\boldsymbol{H}\boldsymbol{F})^{-1}\boldsymbol{F}^H\boldsymbol{H}^H\boldsymbol{F}^{-1}\boldsymbol{H}^\dagger \tag{47}$$

where for the second equality, we relied on (43), for the third, we used the definition of the pseudo-inverse, and for the fourth one, we noted that $\boldsymbol{F}$ is a square full-rank matrix. ■

It is interesting to note that a3) is also satisfied by the special cases described in Section III (some with appropriate modifications). Five remarks are now in order concerning the implications of Theorems 1 and 2 to multicarrier modulations and the FS approaches outlined in Section III-A.

Remark 1: With $P-M=1$, the statement 1.1a of Theorem 1 was also proved in [39]. Notice though that 1.1a is not necessary and sufficient as claimed in [39]. In fact, cases 1.1b and 1.1c confirm that there are pairs $(\boldsymbol{F}_0, \boldsymbol{\mathcal{H}})$ where $\boldsymbol{\mathcal{H}}$ does not meet the requirements of 1.1a, but still, linear equalization is impossible.

Remark 2: In view of result 1.2 in Theorem 1, OFDM precoders with cyclic prefix do not satisfy (30) $\forall\, Q$, no matter low long the cyclic prefix is. Channels with nulls at frequencies $2\pi m/M$ do not admit linear equalizers. However, relying on precoders with trailing zeros and selecting $P - M \geq L$, Theorem 2 suggests a practical modification to the OFDM system, which is important because trailing zeros are adopted in the DAB standard (ETS 400 301) in the form of guard bits.[4] Instead of the cyclic prefix (or suffix), we could pad L trailing zeros (TZ) to the M information bits and thus "break" the

[4]We thank Reviewer 4 for bringing up this interesting link with the DAB standard.

Vandermonde structure of the conventional OFDM precoder in order to achieve with FIR filterbanks (as per Theorem 2) ZF equalization of FIR channels, irrespective of their zeros. Such a modification, which we term TZ-OFDM, alters (15) and yields ZF equalizers even for channels with zeros on the unit circle located at angles $2\pi m/M$. A blind adaptive OFDM equalizer was proposed recently in [6] by forcing zeros in the equalizer output (see also [27]). Our result in Theorem 2 proves that such blind algorithms guarantee channel identifiability, irrespective of the channel zero locations.

Remark 3: Result 1.1c of Theorem 1 shows that aperiodic precoding adds robustness against deep frequency-selective fading. Instead of using purely aperiodic precoders, coding with period QP, where $Q \geq P/(P-M)$, is sufficient. In modern systems such as UMTS, for example [23], the coded data are multiplied by a scrambling code of length greater than the symbol duration to add extra robustness against intercell interference (different base stations use different scrambling codes). Indeed, this operation induces aperiodicity in the precoding. It is interesting to observe, according to Theorem 1, that long period scrambling is also important to guarantee ZF linear equalization, irrespective of the channel zeros.

Remark 4: For spread-spectrum (SS) and CDMA systems, the $f_m(n)$ filters are often selected as pseudo-random codes and satisfy a3) almost surely. The wide spectrum of each code implies that $f_m(n)$ can be expressed as the sum of a large number of complex exponentials, which illustrates that SS codes can be constructed using a particular set of Vandermonde vectors. Within the class of Walsh–Hadamard codes, which is currently considered for third generation cellular systems [23], there are codes that can be decomposed into just a few complex exponentials, and for ZF equalization purposes, we have to check whether a3) is satisfied. As we mentioned in Section III-D, TDMA systems use $f_m(n) = \delta(n-m)$; hence, if $P - M \geq L$, $\boldsymbol{F}_0 = (\boldsymbol{I}_{M\times M}\ \boldsymbol{0}_{M\times(P-M)})^T$ will obey a3). This fact and Theorem 2 corroborate the result in [13] and [18], where a TDMA precoder accepts a ZF equalizer without channel zero restrictions for $P - M \geq L$.

Remark 5: The precoder construction algorithms resulting from Theorems 1 and 2 introduce structured redundancy, parsed into consecutive blocks of data, to allow PR of the transmitted data from finite received samples. Thus, information symbols arriving at rate $1/T_s$ are transmitted at a rate $P/(MT_s)$ with $P > M$, utilizing, much like channel encoding, a wider transmission bandwidth. It is useful to compare this precoding strategy with methods based on fractional sampling (FS) [33], [34]. With FS approaches it is also necessary to use a transmission bandwidth greater than $1/T_s$ (using e.g., root-raised cosine shaping filters with roll-off factors $\alpha > 0$ [24]) because otherwise, channel disparity and, thus, identifiability is impossible [7], [34]. To compare our precoding with FS approaches in terms of excess transmit-bandwidth, it is fair to choose parameters M, L, and α so that the bandwidth increase is identical in both cases. Notwithstanding, the two methods differ considerably in the way redundancy is introduced. With reference to the equivalent scheme for FS reported in Fig. 3(a), $M = 1$ and with $P > 1$, the channel length becomes L_sP; hence, $M = 1$ does not satisfy a1), implying that Theorems 1 and 2 cannot be applied. Therefore, extra channel disparity conditions are required with FS-based methods to guarantee FIR equalization.

V. Optimal Zero-Order Filterbank Transceivers

Having established the conditions for perfect channel equalization, in this section, we optimize jointly the transmit/receive filterbank pair when channel status information is available at the transmitter side, which is a situation that occurs, for example, in applications such as high bit rate (and asymmetric) digital subscriber loops (HDSL/ADSL). Specifically, we suppose that the channel as well as the signal and noise covariance matrices $\boldsymbol{R}_{ss}$ and $\boldsymbol{R}_{vv}$ are given (known or estimated beforehand using e.g., training). In HDSL/ADSL applications, reverse links are used to feed channel status information (namely, $\boldsymbol{H}$ and $\boldsymbol{R}_{vv}$ estimates) back to the transmitter. Furthermore, in most practical scenarios, the transmitted symbols are uncorrelated, and thus, $\boldsymbol{R}_{ss}$ is diagonal and known. When symbols $s(n)$ are correlated, source coding is generally employed to remove this redundancy and produce an independent (and thus uncorrelated) data stream. If symbol correlation is due to channel coding and used for error-correction purposes, the encoder is known, and the covariance matrix of the coded symbols is thus available *a priori*.

We will also adopt the choice $P = M+L$, which leads to the minimum order (i.e., $Q = 1$) and, thus, reduced complexity filterbank equalization. In contrast to Section IV, where the precoder $\boldsymbol{F}_0$ was fixed and the equalizer $\boldsymbol{G}_0$ was obtained for a given noiseless channel, here we will optimize both $\boldsymbol{F}_0$ and $\boldsymbol{G}_0$ jointly, using two different criteria. To minimize noise effects in a symbol-by-symbol detection scheme, we are motivated to minimize the output noise power given by the trace of the noise covariance matrix at the equalizer's output, namely, $\mathrm{tr}(\boldsymbol{G}_0\boldsymbol{R}_{vv}\boldsymbol{G}_0^H)$. Clearly, unconstrained minimization leads to the trivial solution $\boldsymbol{G}_0 \equiv \boldsymbol{0}$, which contradicts the goal of symbol recovery, unless infinite power is transmitted. Hence, we will generalize existing optimality criteria adopted for continuous-time transmit-receive pulse shaping filter design to our discrete-time redundant filterbank-based block transmission scheme of Fig. 1 by imposing the ZF or limited transmit-power constraints.

In the next subsection, we will detail the assumptions and filterbank structures adopted in the optimization of our transmission system and point out their consequences to the I/O block relationship (10). Our FIR channel model contains zeros only and is commonly adopted in radio communication channels induced by multipath propagation [24]. Nevertheless, the optimization derived in this paper can be easily extended to pole-zero channels along the lines of [28], but we will omit this case for brevity.

A. Unified TZ/LZ Block Model

Let assumptions a0)–a2) hold true with $P = M + L$ in a1). As mentioned at the beginning of Section IV, we have under a2) that $\boldsymbol{F}_i = \boldsymbol{F}_0\delta(i)$, $\boldsymbol{G}_j = \boldsymbol{G}_0\delta(j)$ and from a0) that $\boldsymbol{H}_l = \boldsymbol{H}_0\delta(l) + \boldsymbol{H}_1\delta(l-1)$, which together with a1) implies that interblock interference due to the channel entails no more

than two successive blocks, namely, $\boldsymbol{s}(n)$ and $\boldsymbol{s}(n-1)$; thus, (10) becomes

$$\hat{\boldsymbol{s}}(n) = \boldsymbol{G}_0\boldsymbol{H}_0\boldsymbol{F}_0\boldsymbol{s}(n) + \boldsymbol{G}_0\boldsymbol{H}_1\boldsymbol{F}_0\boldsymbol{s}(n-1) + \boldsymbol{G}_0\boldsymbol{v}(n) \quad (48)$$

where, consistent with definitions (6), (7), and (19), matrix $\boldsymbol{F}_0$ is $P\times M$, $\boldsymbol{G}_0$ is $M\times P$, and $\boldsymbol{H}_0$, $\boldsymbol{H}_1$ are square $P\times P$ matrices. Recalling Theorems 1 and 2, for perfect reconstruction (PR) or zero-forcing (ZF) equalization of $\boldsymbol{s}(n)$ from $\hat{\boldsymbol{s}}(n)$, two options can be pursued.

i) Force the last L samples of the transmit filters to be zero so that $\boldsymbol{F}_0 = (\boldsymbol{F}^T \ \ \boldsymbol{0})^T$ with $\boldsymbol{F}$ an $M\times M$ matrix and $\boldsymbol{0}$ an $L\times M$ block of zeros, and let $\boldsymbol{G}_0 = \boldsymbol{G}$, where $\boldsymbol{G}$ is a $M\times P$ matrix [we term this option the trailing transmitter zeros (TZ) approach].

ii) Force the first L filters of the receive filterbank to be zero, so that $\boldsymbol{G}_0 = (\boldsymbol{0} \ \ \boldsymbol{G})$, where now, $\boldsymbol{G}$ is an $M\times M$ matrix, whereas $\boldsymbol{F}_0 = \boldsymbol{F}$ and $\boldsymbol{F}$ has now dimensionality $P\times M$ [correspondingly, we call this option the leading receiver zeros (LZ) approach].

Although the dimensionalities of $\boldsymbol{F}$ and $\boldsymbol{G}$ will vary for options i) and ii), for brevity, we will use a unified notation for both cases because if $\boldsymbol{H}$ is defined appropriately, (48) has a common form

$$\hat{\boldsymbol{s}}(n) = \boldsymbol{G}\boldsymbol{H}\boldsymbol{F}\boldsymbol{s}(n) + \boldsymbol{G}\boldsymbol{v}(n). \quad (49)$$

Specifically, for case i) of trailing transmitter zeros, the matrix $\boldsymbol{H}$ is $P\times M$ and is defined as

$$\boldsymbol{H} = \boldsymbol{H}_{TZ} := \begin{pmatrix} h(0) & 0 & \cdots & 0 \\ \vdots & \ddots & \ddots & \vdots \\ h(L) & \ddots & \ddots & 0 \\ 0 & \ddots & \ddots & h(0) \\ \vdots & \ddots & \ddots & \vdots \\ 0 & \ddots & 0 & h(L) \end{pmatrix} \quad (50)$$

whereas for case ii) of LZ, $\boldsymbol{H}$ denotes the $M\times P$ matrix

$$\boldsymbol{H} = \boldsymbol{H}_{LZ} := \begin{pmatrix} h(L) & \cdots & h(0) & 0 & \cdots & 0 \\ 0 & \ddots & \ddots & \ddots & \cdots & \vdots \\ \vdots & \vdots & \ddots & \ddots & \ddots & 0 \\ 0 & \cdots & 0 & h(L) & \cdots & h(0) \end{pmatrix}. \quad (51)$$

Moreover, vector $\boldsymbol{v}(n)$ has length P in TZ and M in the LZ case. We will also assume the following.

a4) Input $\boldsymbol{s}(n)$ and AGN $\boldsymbol{v}(n)$ are mutually uncorrelated, stationary with known covariance matrices $\boldsymbol{R}_{ss}$ ($M\times M$) and $\boldsymbol{R}_{vv}$ ($P\times P$ in the TZ and $M\times M$ in the LZ case), respectively ($\sigma_{ss}^2\boldsymbol{I}$ and $\sigma_{vv}^2\boldsymbol{I}$ when white).

Allowing colored inputs accounts for coded transmissions (see e.g., [20]), whereas color at the receiver noise incorporates cross-talk, interchannel interference, and residual echo.

B. ZF Constrained Output SNR Criterion

Based on (49), which applies to both TZ and LZ alternatives, we formulate our max-SNR/ZF constrained optimization problem as follows. We wish to satisfy the ZF constraint $\boldsymbol{G}\boldsymbol{H}\boldsymbol{F} = \mathcal{K}\boldsymbol{I}_{M\times M}$, whereas at the same time maximize the SNR at the equalizer output, which is defined as

$$\begin{aligned}\text{SNR} &= \frac{\text{tr}(E\{\boldsymbol{G}\boldsymbol{H}\boldsymbol{F}\boldsymbol{s}(n)\boldsymbol{s}^H(n)\boldsymbol{F}^H\boldsymbol{H}^H\boldsymbol{G}^H\})}{\text{tr}(E\{\boldsymbol{G}\boldsymbol{v}(n)\boldsymbol{v}(n)^H\boldsymbol{G}^H\})} \\ &= \frac{\text{tr}(\boldsymbol{G}\boldsymbol{H}\boldsymbol{F}\boldsymbol{R}_{ss}\boldsymbol{F}^H\boldsymbol{H}^H\boldsymbol{G}^H)}{\text{tr}(\boldsymbol{G}\boldsymbol{R}_{vv}\boldsymbol{G}^H)}\end{aligned}$$

and, in view of the ZF condition, becomes

$$\text{SNR} = \frac{\mathcal{K}^2\,\text{tr}(\boldsymbol{R}_{ss})}{\text{tr}(\boldsymbol{G}\boldsymbol{R}_{vv}\boldsymbol{G}^H)}.$$

Because the numerator is a constant, we write it as $\mathcal{K}^2|\text{tr}(\boldsymbol{I}_{M\times M})|^2$ to point out the dependence on the block-length M and the contribution of the (generally complex) transmit-amplification gain $\mathcal{K}$ whose magnitude $|\mathcal{K}| > 0$ depends on the transmitted power and controls the SNR at the equalizer output. Because SNR is only magnitude dependent, we take, without loss of generality (w.l.o.g.), $\mathcal{K}$ to be real and positive. Our max-SNR/ZF constrained optimization problem can now be formulated as

$$\max_{\boldsymbol{G},\boldsymbol{F}} \mathcal{K}^2\,\frac{|\text{tr}(\boldsymbol{I}_{M\times M})|^2}{\text{tr}(\boldsymbol{G}\boldsymbol{R}_{vv}\boldsymbol{G}^H)} \quad \text{subject to} \quad \boldsymbol{G}\boldsymbol{H}\boldsymbol{F} = \mathcal{K}\boldsymbol{I}_{M\times M}. \quad (52)$$

A related criterion was adopted in the continuous-time scalar pulse-shaper design by [12]. It turns out that (52) is equivalent to minimizing the output mean square error subject to the ZF constraint. To solve (52) in our vector equalizer setup, we use the trace to define the (weighted) inner-product between two matrices $\boldsymbol{A}$, $\boldsymbol{B}$ as $(\boldsymbol{A},\boldsymbol{B})_{\boldsymbol{W}} := \text{tr}(\boldsymbol{A}^H\boldsymbol{W}\boldsymbol{B})$, where $\boldsymbol{W}$ is a positive-definite Hermitian matrix. Using this definition, Schwartz's inequality shows that SNR in (52) obeys

$$\begin{aligned}\frac{|\text{tr}(\boldsymbol{I}_{M\times M})|^2}{\text{tr}(\boldsymbol{G}\boldsymbol{R}_{vv}\boldsymbol{G}^H)} &\equiv \frac{|(\boldsymbol{G}^H, \boldsymbol{R}_{vv}^{-1}\boldsymbol{H}\boldsymbol{F})_{\boldsymbol{R}_{vv}}|^2}{(\boldsymbol{G}^H,\boldsymbol{G}^H)_{\boldsymbol{R}_{vv}}} \\ &\le (\boldsymbol{R}_{vv}^{-1}\boldsymbol{H}\boldsymbol{F},\boldsymbol{R}_{vv}^{-1}\boldsymbol{H}\boldsymbol{F})_{\boldsymbol{R}_{vv}}\end{aligned}$$

and is maximized if and only if, for some complex constant α, we have $\boldsymbol{G}^H = \alpha^*\boldsymbol{R}_{vv}^{-1}\boldsymbol{H}\boldsymbol{F}$, or

$$\boldsymbol{G} = \alpha\boldsymbol{F}^H\boldsymbol{H}^H\boldsymbol{R}_{vv}^{-1}. \quad (53)$$

If $\boldsymbol{v}(n)$ is white, then $\boldsymbol{G} = (\alpha/\sigma_v^2)\boldsymbol{F}^H\boldsymbol{H}^H$, and in order to simplify subsequent expressions, we select $\alpha = \sigma_v^2$. Using this choice for α in (53), our ZF constraint in (52) becomes

$$\boldsymbol{F}^H\boldsymbol{H}^H\boldsymbol{R}_{vv}^{-1}\boldsymbol{H}\boldsymbol{F} = \frac{\mathcal{K}}{\sigma_v^2}\boldsymbol{I}_{M\times M}. \quad (54)$$

Solving for the optimum $\boldsymbol{G}_{opt}$ and $\boldsymbol{F}_{opt}$ from (53) and (54) depends on whether leading or trailing zeros are forced in the equalizer or in the precoder filterbank. However, adopting the conventions described in Section V-A, we express the solution for both cases in a unified form as follows.

Theorem 3—Max-SNR/ZF Equalizers: Let assumptions a0)–a2) and a4) hold true, and let the channel matrix $\boldsymbol{H}$ be as in (50) or (51). Denoting by $\boldsymbol{U}$, $\boldsymbol{V}$, $\boldsymbol{V}_n$ the unitary matrices and by $\boldsymbol{\Delta}$, $\boldsymbol{\Lambda}$ the diagonal matrices[5] resulting from the eigendecompositions

$$\begin{aligned} \boldsymbol{R}_{ss} &= \boldsymbol{U}\boldsymbol{\Delta}\boldsymbol{U}^H \\ \boldsymbol{H}^H\boldsymbol{R}_{vv}^{-1}\boldsymbol{H} &= \begin{cases} \boldsymbol{V}\boldsymbol{\Lambda}\boldsymbol{V}^H & \text{(TZ)} \\ (\boldsymbol{V}, \boldsymbol{V}_n)\begin{pmatrix} \boldsymbol{\Lambda} & \boldsymbol{0} \\ \boldsymbol{0} & \boldsymbol{0} \end{pmatrix}(\boldsymbol{V}, \boldsymbol{V}_n)^H & \text{(LZ)} \end{cases} \end{aligned} \tag{55}$$

the output SNR in (52) is maximized by the optimum ZF $(\boldsymbol{F}, \boldsymbol{G})$ pair of filterbanks

$$\begin{aligned} \boldsymbol{F}_{opt} &= \frac{\sqrt{\mathcal{K}}}{\sigma_v}\boldsymbol{V}\boldsymbol{\Lambda}^{-(1/2)} \\ \boldsymbol{G}_{opt} &= \sigma_v\sqrt{\mathcal{K}}\boldsymbol{\Lambda}^{-(1/2)}\boldsymbol{V}^H\boldsymbol{H}^H\boldsymbol{R}_{vv}^{-1}. \end{aligned} \tag{56}$$

Proof: By direct substitution, $(\boldsymbol{F}_{opt}, \boldsymbol{G}_{opt})$ of (56) satisfy (53) and (54) and, thus, achieve optimality in the sense of (52). ■

Interesting special cases appear when $\boldsymbol{v}(n)$ is white with variance σ_v^2. In this case, it suffices to replace $\boldsymbol{\Lambda}$ with $\sigma_v^2\boldsymbol{\Lambda}$ in (56) to obtain

$$\boldsymbol{F}_{opt} = \sqrt{\mathcal{K}}\boldsymbol{V}\boldsymbol{\Lambda}^{-(1/2)}, \qquad \boldsymbol{G}_{opt} = \sqrt{\mathcal{K}}\boldsymbol{U}_h^H \tag{57}$$

where $\boldsymbol{U}_h$ is found from the SVD $\boldsymbol{H} = \boldsymbol{U}_h\boldsymbol{\Lambda}^{1/2}\boldsymbol{V}^H$. In (57), the optimum precoder (equalizer) filterbank matrices are proportional to the left (right) singular vectors of the channel matrix. Transmitter filterbanks are also weighted by the inverse of the square root of the corresponding singular values.

It is interesting to observe that the matrix $\boldsymbol{G}_{opt}$ not only guarantees (together with $\boldsymbol{F}_{opt}$) the ZF condition but also provides uncorrelated noise samples at its output. Indeed, the covariance matrix of the output noise $\boldsymbol{G}_{opt}\boldsymbol{v}(n)$ is $\boldsymbol{G}_{opt}\boldsymbol{R}_{vv}\boldsymbol{G}_{opt}^H = \mathcal{K}\sigma_v^2\boldsymbol{I}$.

Remark 6: With flat fading (the channel matrix is diagonal) and white noise, (57) yields precoder and equalizer filterbanks with diagonal structure. Recalling from Section III that TDMA corresponds to $f_m(n) = \delta(n-m)$, we infer that TDMA possesses optimality (in the ZF maximum output SNR sense) when it comes to channels involving flat fading and white noise.

C. Constrained Mean-Square Error Criterion

The ultimate objective in digital communications is to minimize error probability, and although maximizing output SNR under the ZF constraint leads to a simple closed-form solution, alternative criteria allowing for residual ISI may come closer to the desired goal. One such candidate is the minimum mean-square error (MMSE) criterion, which minimizes $\mathcal{E} := E\{\text{tr}(\boldsymbol{e}(n)\boldsymbol{e}^H(n))\}$, where $\boldsymbol{e}(n) := \hat{\boldsymbol{s}}(n) - \boldsymbol{s}(n)$ is the error in the nth data block. Based on (49), we find

$$\boldsymbol{e}(n) = \boldsymbol{G}\boldsymbol{y}(n) - \boldsymbol{s}(n) = \boldsymbol{G}\boldsymbol{H}\boldsymbol{F}\boldsymbol{s}(n) + \boldsymbol{G}\boldsymbol{v}(n) - \boldsymbol{s}(n) \tag{58}$$

and using (58), the MSE objective function becomes

$$\begin{aligned} \mathcal{E}(\boldsymbol{F}, \boldsymbol{G}) = &\text{tr}((\boldsymbol{G}\boldsymbol{H}\boldsymbol{F} - \boldsymbol{I})\boldsymbol{R}_{ss}(\boldsymbol{G}\boldsymbol{H}\boldsymbol{F} - \boldsymbol{I})^H) \\ &+ \text{tr}(\boldsymbol{G}\boldsymbol{R}_{vv}\boldsymbol{G}^H). \end{aligned} \tag{59}$$

Without any constraint, minimizing $\mathcal{E}$ leads to the trivial solution corresponding to $\|\boldsymbol{G}\| = 0$ and requiring infinite power to be transmitted $\|\boldsymbol{F}\| = \infty$. A reasonable constraint that takes into account limited budget resources is the transmitted power, which is expressed as $P_0 := \text{tr}(\boldsymbol{F}\boldsymbol{R}_{ss}\boldsymbol{F}^H)$. With the transmit-power constrained, our criterion becomes

$$\min_{\boldsymbol{F}, \boldsymbol{G}} \mathcal{E}(\boldsymbol{F}, \boldsymbol{G}) \quad \text{subject to} \quad \mathcal{C} := \text{tr}(\boldsymbol{F}\boldsymbol{R}_{ss}\boldsymbol{F}^H) - P_0 = 0. \tag{60}$$

Analogous criteria formulated in the frequency-domain for joint transmit/receive-filter optimization can be found in the scalar case (e.g., [2, p. 333]) or in the more challenging multi-input–multi-output case in [40]. Optimizing our criterion in (60) follows the steps in [40], but our discrete time-domain matrix formulation will lead to a *closed-form* selection of the redundant FIR filterbank matrices (redundancy was not exploited in [40], and IIR frequency-domain designs were optimized via *iterative* minimization of Lagrange multipliers).

From (59), using the method of Lagrange multipliers, the objective function can be written as

$$\begin{aligned} \mathcal{E} + \mu\mathcal{C} = &\text{tr}((\boldsymbol{G}\boldsymbol{H}\boldsymbol{F} - \boldsymbol{I})\boldsymbol{R}_{ss}(\boldsymbol{G}\boldsymbol{H}\boldsymbol{F} - \boldsymbol{I})^H) \\ &+ \text{tr}(\boldsymbol{G}\boldsymbol{R}_{vv}\boldsymbol{G}^H) + \mu(\text{tr}(\boldsymbol{F}\boldsymbol{R}_{ss}\boldsymbol{F}^H) - P_0). \end{aligned} \tag{61}$$

Differentiating with respect to $\boldsymbol{G}$, we find

$$\nabla_{\boldsymbol{G}}(\mathcal{E} + \mu\mathcal{C}) = 2\boldsymbol{R}_{vv}\boldsymbol{G}^H + 2\boldsymbol{H}\boldsymbol{F}\boldsymbol{R}_{ss}(\boldsymbol{G}\boldsymbol{H}\boldsymbol{F} - \boldsymbol{I})^H = \boldsymbol{0} \tag{62}$$

which can be solved for $\boldsymbol{G}$ to obtain

$$\boldsymbol{G} = \boldsymbol{R}_{ss}\boldsymbol{F}^H\boldsymbol{H}^H(\boldsymbol{R}_{vv} + \boldsymbol{H}\boldsymbol{F}\boldsymbol{R}_{ss}\boldsymbol{F}^H\boldsymbol{H}^H)^{-1}. \tag{63}$$

Differentiating with respect to $\boldsymbol{F}$, we find

$$\nabla_{\boldsymbol{F}}(\mathcal{E} + \mu\mathcal{C}) = 2\boldsymbol{R}_{ss}(\boldsymbol{G}\boldsymbol{H}\boldsymbol{F} - \boldsymbol{I})^H\boldsymbol{G}\boldsymbol{H} + 2\mu\boldsymbol{R}_{ss}\boldsymbol{F}^H = \boldsymbol{0} \tag{64}$$

which can be solved for $\boldsymbol{F}$ to obtain

$$\boldsymbol{F} = (\boldsymbol{H}^H\boldsymbol{G}^H\boldsymbol{G}\boldsymbol{H} + \mu\boldsymbol{I})^{-1}\boldsymbol{H}^H\boldsymbol{G}^H. \tag{65}$$

It is evident that solving (65) and (63) for $\boldsymbol{F}$ and $\boldsymbol{G}$ and using the constraint $\text{tr}(\boldsymbol{F}\boldsymbol{R}_{ss}\boldsymbol{F}^H) = P_0$ is not an easy task. To tackle the problem, we will simplify the objective function by diagonalizing the symmetric matrices involving $\boldsymbol{R}_{ss}$, $\boldsymbol{H}$, $\boldsymbol{R}_{vv}$, all of which are assumed to be available. Toward this end, we first find the unitary matrices $\boldsymbol{U}$, $\boldsymbol{V}$, and the diagonal matrices $\boldsymbol{\Delta}$, $\boldsymbol{\Lambda}$ from the eigendecompositions in (55). Next, with appropriately defined matrices $\boldsymbol{\Phi}$ and $\boldsymbol{\Gamma}$, we focus on matrices $\boldsymbol{F}$ and $\boldsymbol{G}$ that can be decomposed as

$$\boldsymbol{F} = \boldsymbol{V}\boldsymbol{\Phi}\boldsymbol{U}^H, \qquad \boldsymbol{G} = \boldsymbol{U}\boldsymbol{\Gamma}\boldsymbol{\Lambda}^{-1}\boldsymbol{V}^H\boldsymbol{H}^H\boldsymbol{R}_{vv}^{-1}. \tag{66}$$

Clearly, when $\boldsymbol{F}$ and $\boldsymbol{G}$ are $M \times M$ square matrices ($\boldsymbol{F}$ in TZ and $\boldsymbol{G}$ in LZ), the decompositions in (66) impose no

[5] In the LZ case, the matrix $\boldsymbol{H}^H\boldsymbol{R}_{vv}^{-1}\boldsymbol{H}$ is singular, and $\boldsymbol{\Lambda}$ and $\boldsymbol{V}$ have to be formed by the nonzero eigenvalues and the corresponding eigenvector matrices (of dimensionality $M \times M$ and $P \times M$, respectively), rather than the full matrices eigendecomposing $\boldsymbol{H}^H\boldsymbol{R}_{vv}^{-1}\boldsymbol{H}$. Note that if the optimization is also constrained by the transmit power P_0, (56) does not provide the max-SNR/ZF filterbank transceivers; the optimum pair in this case turns out to be $\boldsymbol{F}_{opt} = [P_0/\text{tr}(\boldsymbol{\Lambda}^{-1/2})]^{1/2}\boldsymbol{V}\boldsymbol{\Lambda}^{-1/4}$, $\boldsymbol{G}_{opt} = \boldsymbol{F}_{opt}^{-1}\boldsymbol{H}^\dagger$ (see also Theorem 4 for a constrained-power MMSE solution).

restriction in our optimization search. However, even when $\boldsymbol{F}$ is tall ($P \times M$ in LZ) or when $\boldsymbol{G}$ is fat ($M \times P$ in TZ), our decompositions in (66) still impose no loss of generality[6] when it comes to minimizing $\mathcal{E}$ under the power constraint $\mathcal{C}$. Indeed, if for the LZ case we augment $\boldsymbol{F} \in \mathcal{R}(\boldsymbol{V})$ by its orthogonal complement in $\mathcal{N}(\boldsymbol{V})$ to obtain the most general decomposition $\overline{\boldsymbol{F}} = \boldsymbol{V}\boldsymbol{\Phi}\boldsymbol{U}^H + \boldsymbol{V}_n\boldsymbol{\Phi}_n\boldsymbol{U}^H = \boldsymbol{F} + \boldsymbol{V}_n\boldsymbol{\Phi}_n\boldsymbol{U}^H$, it follows by direct substitution that $\boldsymbol{G}\boldsymbol{H}\overline{\boldsymbol{F}} = \boldsymbol{G}\boldsymbol{H}\boldsymbol{F} + \boldsymbol{G}\boldsymbol{H}\boldsymbol{V}_n\boldsymbol{\Phi}_n\boldsymbol{U}^H = \boldsymbol{G}\boldsymbol{H}\boldsymbol{F}$ since $\boldsymbol{V}_n$ is the right null space of $\boldsymbol{H}$ [c.f. (55)]; thus, $\mathcal{E}(\overline{\boldsymbol{F}}, \boldsymbol{G}) = \mathcal{E}(\boldsymbol{F}, \boldsymbol{G})$, and our choice in (66) does not alter the MSE. However, $\mathrm{tr}(\overline{\boldsymbol{F}}\boldsymbol{R}_{ss}\overline{\boldsymbol{F}}^H) = \mathrm{tr}(\boldsymbol{F}\boldsymbol{R}_{ss}\boldsymbol{F}^H) + \mathrm{tr}(\boldsymbol{\Phi}_n\boldsymbol{R}_{ss}\boldsymbol{\Phi}_n^H) \geq \mathrm{tr}(\boldsymbol{F}\boldsymbol{R}_{ss}\boldsymbol{F}^H)$, which implies $\mathcal{C}(\overline{\boldsymbol{F}}) \geq \mathcal{C}(\boldsymbol{F})$, i.e., incorporating $\boldsymbol{V}_n\boldsymbol{\Phi}_n\boldsymbol{U}^H$ violates the power constraint unless $\boldsymbol{\Phi}_n \equiv \boldsymbol{0}$, which corresponds to selecting $\overline{\boldsymbol{F}}$ equal to $\boldsymbol{F}$ in (66). Similarly, if for the TZ case we add the orthogonal complement of $\mathcal{R}(\boldsymbol{H}^H\boldsymbol{R}_{vv}^{-1/2})$ to obtain the most general receive filterbank $\overline{\boldsymbol{G}} = \boldsymbol{G} + \boldsymbol{U}\boldsymbol{\Gamma}\boldsymbol{\Lambda}^{-1}\boldsymbol{V}^H(\boldsymbol{I} - \boldsymbol{R}_{vv}^{-1/2}\boldsymbol{H}(\boldsymbol{H}\boldsymbol{R}_{vv}^{-1}\boldsymbol{H}^H)^{-1}\boldsymbol{H}^H\boldsymbol{R}_{vv}^{-1/2})\boldsymbol{R}_{vv}^{-1/2}$, then it can be easily verified that $\overline{\boldsymbol{G}}\boldsymbol{H}\boldsymbol{F} = \boldsymbol{G}\boldsymbol{H}\boldsymbol{F}$, but $\mathrm{tr}(\overline{\boldsymbol{G}}\boldsymbol{R}_{vv}\overline{\boldsymbol{G}}^H) \geq \mathrm{tr}(\boldsymbol{G}\boldsymbol{R}_{vv}\boldsymbol{G}^H)$ with equality holding if and only if $\overline{\boldsymbol{G}} \equiv \boldsymbol{G}$, i.e., incorporating the null space of $\boldsymbol{H}^H\boldsymbol{R}_{vv}^{-1/2}$ leads to $\mathcal{E}(\boldsymbol{F}, \overline{\boldsymbol{G}}) \geq \mathcal{E}(\boldsymbol{F}, \boldsymbol{G})$ unless $\overline{\boldsymbol{G}}$ equals our $\boldsymbol{G}$ in (66).

Using (66), we show in the Appendix that the objective function in (61) can be written as

$$\begin{aligned}\mathcal{E}(\boldsymbol{\Gamma}, \boldsymbol{\Phi}) + \mu\mathcal{C}(\boldsymbol{\Phi}) &= \mathrm{tr}(\boldsymbol{\Gamma}\boldsymbol{\Lambda}^{-1}\boldsymbol{\Gamma}^H) + \mathrm{tr}((\boldsymbol{\Gamma}\boldsymbol{\Phi} - \boldsymbol{I})\boldsymbol{\Delta}(\boldsymbol{\Gamma}\boldsymbol{\Phi} - \boldsymbol{I})^H) \\ &\quad + \mu(\mathrm{tr}(\boldsymbol{\Phi}\boldsymbol{\Delta}\boldsymbol{\Phi}^H) - P_0). \end{aligned} \tag{67}$$

Differentiating with respect to $\boldsymbol{\Gamma}$ and $\boldsymbol{\Phi}$ and equating the results to zero, we arrive at

$$\boldsymbol{\Gamma} = \boldsymbol{\Delta}\boldsymbol{\Phi}^H(\boldsymbol{\Lambda}^{-1} + \boldsymbol{\Phi}\boldsymbol{\Delta}\boldsymbol{\Phi}^H)^{-1} \tag{68}$$

$$\boldsymbol{\Phi} = (\boldsymbol{\Gamma}^H\boldsymbol{\Gamma} + \mu\boldsymbol{I})^{-1}\boldsymbol{\Gamma}^H. \tag{69}$$

Relying on (68) and (69), the objective in (67) can be further simplified based on the following lemma (see the Appendix for proofs):

Lemma: Matrices $\boldsymbol{\Gamma}^H\boldsymbol{\Gamma}$, $\boldsymbol{\Phi}\boldsymbol{\Delta}\boldsymbol{\Phi}^H$, and $\boldsymbol{\Phi}\boldsymbol{\Delta}^2\boldsymbol{\Phi}^H$ are diagonal.

Using this Lemma, we prove in the Appendix that, w.l.o.g., $\boldsymbol{\Phi}$ can be assumed to be diagonal and that (67) is equivalent to

$$\min_{\phi_{ii}}(\mathcal{E} + \mu\mathcal{C}) = \min_{\phi_{ii}}\left(\sum_i \frac{\delta_{ii}}{1 + |\phi_{ii}|^2\delta_{ii}\lambda_{ii}} + \mu\left(\sum_i |\phi_{ii}|^2\delta_{ii} - P_0\right)\right) \tag{70}$$

where $\phi_{ii}(\delta_{ii}, \lambda_{ii})$ denotes the (i, i)th entry of $\boldsymbol{\Phi}(\boldsymbol{\Delta}, \boldsymbol{\Lambda})$. Setting $\partial(\mathcal{E} + \mu\mathcal{C})/\partial\phi_{ii} = 0$ and solving with respect to $|\phi_{ii}|^2$, we find

$$|\phi_{ii}|^2 = \sqrt{\frac{\lambda_{ii}^{-1}}{\mu\delta_{ii}}} - \frac{\lambda_{ii}^{-1}}{\delta_{ii}}. \tag{71}$$

[6]Clarification of these "tall $\boldsymbol{F}$/ fat $\boldsymbol{G}$ cases," as well as our comments on "channels with repeated eigenvalues" in the footnote of the Appendix, were motivated by questions raised by Prof. P. Stoica, whom we also wish to thank for his interest in our work.

Substituting (71) into the constraint $\sum_i |\phi_{ii}|^2\delta_{ii} = P_0$ and solving with respect to μ, we obtain

$$\sqrt{\mu} = \frac{\mathrm{tr}(\boldsymbol{\Lambda}^{-(1/2)}\boldsymbol{\Delta}^{1/2})}{P_0 + \mathrm{tr}(\boldsymbol{\Lambda}^{-1})}. \tag{72}$$

Plugging (72) back to (71) yields

$$|\phi_{ii}|^2 = \frac{P_0 + \mathrm{tr}(\boldsymbol{\Lambda}^{-1})}{\mathrm{tr}(\boldsymbol{\Lambda}^{-(1/2)}\boldsymbol{\Delta}^{1/2})}\frac{1}{\sqrt{\lambda_{ii}\delta_{ii}}} - \frac{1}{\lambda_{ii}\delta_{ii}}. \tag{73}$$

In summary, we have established the following result (and corresponding design algorithm):

Theorem 4—Constrained Power-MMSE Equalizer: Let a0)–a4) hold true with $P = M + L$. Let also the channel matrix $\boldsymbol{H}$ be given and the diagonal matrices $\boldsymbol{\Delta}$ ($\boldsymbol{\Lambda}$) determined from (55) have their diagonal entries in decreasing order. Define the diagonal matrix $\boldsymbol{\Phi}$ with (i, i) entry as in (73). The optimum $(\boldsymbol{F}, \boldsymbol{G})$ filterbank pair in the sense of (60) is given by [see also (66)]

$$\begin{aligned}\boldsymbol{F}_{opt} &= \boldsymbol{V}\boldsymbol{\Phi}\boldsymbol{U}^H \\ \boldsymbol{G}_{opt} &= \boldsymbol{R}_{ss}\boldsymbol{F}_{opt}^H\boldsymbol{H}^H(\boldsymbol{R}_{vv} + \boldsymbol{H}\boldsymbol{F}_{opt}\boldsymbol{R}_{ss}\boldsymbol{F}_{opt}^H\boldsymbol{H}^H)^{-1}. \end{aligned} \tag{74}$$

Assumption a2) in Theorem 4 requires $\mathrm{rank}(\boldsymbol{F}) = M$, which, under the fixed power constraint in (60), imposes the following lower bound on P_0:

$$P_0 > \frac{\mathrm{tr}(\boldsymbol{\Lambda}^{-(1/2)}\boldsymbol{\Delta}^{1/2})}{\sqrt{\min_i(\lambda_{ii}\delta_{ii})}} - \mathrm{tr}(\boldsymbol{\Lambda}^{-1}). \tag{75}$$

In fact, from (71), $|\phi_{ii}|^2 > 0$ only if

$$\min\left(\frac{\delta_{ii}}{\lambda_{ii}^{-1}}\right) > \mu \tag{76}$$

which leads to (75). Lower MMSE values may be reached only if we use less than M branches of the filterbank of Fig. 1 for transmission, which corresponds to additional redundancy introduced to the incoming information stream.

It is noteworthy that according to (74), the overall precoder/channel/equalizer matrix becomes $\boldsymbol{G}_{opt}\boldsymbol{H}\ \boldsymbol{F}_{opt} = \boldsymbol{U}\boldsymbol{\Delta}\boldsymbol{\Phi}\boldsymbol{\Lambda}(\boldsymbol{I} + \boldsymbol{\Lambda}\boldsymbol{\Phi}^2\boldsymbol{\Delta})^{-1}\boldsymbol{\Phi}\boldsymbol{U}^H$. Therefore, the choice (74) converts the channel into the cascade of

i) an encoder matrix $\boldsymbol{U}^H$, which decorrelates the input symbols;
ii) a matrix $\boldsymbol{\Delta}\boldsymbol{\Phi}\boldsymbol{\Lambda}(\boldsymbol{I} + \boldsymbol{\Lambda}\boldsymbol{\Phi}^2\boldsymbol{\Delta})^{-1}\boldsymbol{\Phi}$, which is clearly diagonal;
iii) a decoder matrix $\boldsymbol{U}$.

For uncorrelated input symbols, both optimization criteria diagonalize the channel, which renders block transmission over dispersive channels equivalent to transmission over parallel nondispersive (flat fading) subchannel—a feature establishing links of our transceiver designs in (74) with the well known "water-pouring" principle in information theory (for details see [28] and references therein). The main difference between the two criteria lies on how they allocate power across the parallel subchannels.

Two additional remarks are now in order:

Remark 7: In the existing modulation schemes of Section III, the precoder matrix $\boldsymbol{F}$ is fixed, and in order to minimize MSE, the designer is only free to select the equalizer filterbank $\boldsymbol{G}$. MMSE (or Wiener) equalizing filterbanks in this case are also given by (74), provided that $\boldsymbol{F}_{opt}$ is replaced by the fixed precoder $\boldsymbol{F}$. Note that in (74), equalizing filterbanks consist of a prewhitener (given by the inverse matrix) followed by a filterbank matched to the cascade of the precoder with the channel (corresponding to the term $\boldsymbol{F}^H\boldsymbol{H}^H$). Detailed study of such MMSE equalizers will be reported in a companion paper [27], along with blind synchronization, channel estimation, and direct equalization algorithms.

Remark 8: In this section, joint optimization was carried out in the discrete-time equivalent model assuming transmission with Nyquist pulses. However, from our $(\boldsymbol{F}_{opt}, \boldsymbol{G}_{opt})$ pairs, the continuous-time pulse shaping and receiving filters $\{f_m(t), g_p(t)\}$ are not specified uniquely. Nevertheless, if the $\{f_{m,opt}(t),\ g_{p,opt}(t)\}$ filters are constrained to be bandlimited over $[-\pi P/(MT_s'), \pi P/(MT_s')]$, they can be reconstructed by interpolating our discrete-time optimal solutions $\{f_{m,opt}(n), g_{p,opt}(n)\}$ using the sinc functions. On the other hand, selecting $\{f_m(t), g_p(t)\}$ in the general case requires separate optimization in the continuous-time (or frequency) domain similar to that in [40]. This could be an interesting direction for future research, but the solution may not lead to the simple closed-form FIR designs of this section.

VI. Performance and Simulations

When $\boldsymbol{v}(n)$ in (49) is Gaussian, theoretical probability of error expressions can be derived for the FIR ZF equalizer filterbanks. With $\boldsymbol{\eta}(n) = \boldsymbol{G}\boldsymbol{v}(n)$ denoting the noise at the equalizer output and a q-level symbol constellation, detection based on (49) amounts to a q^M-ary hypotheses testing problem in AGN $\boldsymbol{\eta}(n)$ with covariance $\boldsymbol{R}_{\eta\eta} = \boldsymbol{G}\boldsymbol{R}_{vv}\boldsymbol{G}^H$. To avoid such an exponentially complex problem, we are motivated to consider block-by-block detection, relying on a variant of (49)

$$\hat{\boldsymbol{s}}(n) = \mathcal{K}\boldsymbol{s}(n) + \boldsymbol{G}\boldsymbol{v}(n). \tag{77}$$

To provide a global performance measure per symbol, we adopt the average error probability defined as

$$\overline{P}_e = \frac{1}{M}\sum_{m=0}^{M-1} P_e^{(m)} \tag{78}$$

where $P_e^{(m)}$ denotes the error probability of the mth symbol. For BPSK constellations, the symbol error performance in AGN is

$$P_e^{(m)} = \frac{1}{2}\,\mathrm{erfc}\left(\frac{\mathcal{K}}{\sqrt{\boldsymbol{g}_m^H\boldsymbol{R}_{vv}\boldsymbol{g}_m}}\right) \tag{79}$$

where $\boldsymbol{g}_m^H$ is the mth row of the receiver matrix $\boldsymbol{G}$. Generalizations of (79) to larger constellations follow along known lines [2, p. 140]. If the optimum ZF equalizer is used, it turns out that $\boldsymbol{R}_{\eta\eta} = \sigma_v^2\mathcal{K}\boldsymbol{I}$, revealing that ZF equalizers perform also noise whitening that renders symbol-by-symbol detection optimal. Because $\boldsymbol{g}_m^H\boldsymbol{R}_{vv}\boldsymbol{g}_m = \sigma_v^2\mathcal{K}\boldsymbol{I}$ in this case, we find from (78) and (79) that $P_e^{(m)} = 0.5\,\mathrm{erfc}(\sqrt{\mathcal{K}}/\sigma_v) = \overline{P}_e\ \forall m$.

To illustrate salient features of our designs and to study and compare MMSE designs, we resorted to simulation examples.

Example 1: To check the validity of Theorem 2, we considered an OFDM system with $P = M + L$. Specifically, we implemented the system in Fig. 1 with $M = 32$ and $P = 36$ for an FIR channel of order $L = 4$ with zeros at 1, $0.9\exp(j9\pi/20)$, $1.1\exp(-j9\pi/20)$, and -0.8. We used the OFDM precoder in (11) with $\overline{L} = 4$ and our modification with trailing zeros (term it TZ-OFDM), as described in Theorem 2. Fig. 5(a) shows the BER computed for BPSK $s(n)$ using (78) and (79), which is achieved by using the standard OFDM receiver [which assumes perfect knowledge of the channel and inverts (15)] and our TZ-OFDM receiver in (44). The BER is sketched as a function of E_b/N_0 (dB), where $E_b = E_s$ is the average energy per symbol (bit), i.e., $E_s = (1/M)\sum_{m=1}^{M}\boldsymbol{f}_m^H\boldsymbol{f}_m$, and N_0 is the noise spectral density. As expected, the presence of the channel zero on the unit circle degrades performance of OFDM when compared with TZ-OFDM, which, according to Theorem 2, guarantees the ZF property, irrespective of the channel zeros. In fact, from Fig. 5(a), we notice that as E_b/N_0 increases, TZ-OFDM improves its performance, whereas conventional OFDM incurs a consistent number of symbol errors due to the channel fades so that the corresponding curve in Fig. 5(a) levels off.

To verify results 1.1a and 1.1c of Theorem 1, we considered the case $L = 2$, $M = 7$, and $P = M + 1 < M + L$ and simulated a channel with zeros at 1 and $\exp(j2\pi/P)$. We used a $P \times M$ precoding matrix with its M columns given by the Pth-order Hadamard vectors (the first Hadamard code, i.e., the constant one has been discarded). The corresponding BER, averaged over all the users, is reported in Fig. 5(b) (solid line) where, as predicted by Theorem 1, we observe that the BER curve levels off, corroborating that in this case, it is not possible to invert the matrix $\mathcal{H}\mathcal{F}$ in spite of the spectral richness of the adopted codes. This result is also in agreement with what predicted in [39]. However, using 1.1c of Theorem 1, we know that we can recover from this situation by breaking the periodicity of the code. Specifically, we simulated a system with the same parameters as before and then applied a scrambling code, of length $QP = 2P$, to the coded data by simply multiplying the precoded vector $\mathcal{F}\bar{\boldsymbol{s}}(n)$ with $\mathrm{diag}(\boldsymbol{\theta})$, where $\boldsymbol{\theta}$ is a $2P \times 1$ vector containing a pseudo-noise binary $\{1, -1\}$ code. The corresponding result is reported in Fig. 5(b) and testifies to the gain achieved with the scrambling that corresponds to aperiodic precoding.

According to result 1.2 of Theorem 1 and Remark 2 in Section IV, ZF equalization is not possible for channels with zeros at $\exp(j2\pi l/M)$, with l integer, if the precoding matrix has a cyclic prefix. However, result 1.1c of Theorem 1 shows that a proper aperiodic precoding guarantees perfect equalization for such channels as well. To provide numerical evidence of this statement, we considered the case of $P = M + 2$, $L = 4$, and $Q = 2$. In Fig. 5(c), we report the average BER for plain OFDM with cyclic prefix (solid line B) and the same precoder followed by complex scrambling with period QP (dashed line B). In the same figure, we verify

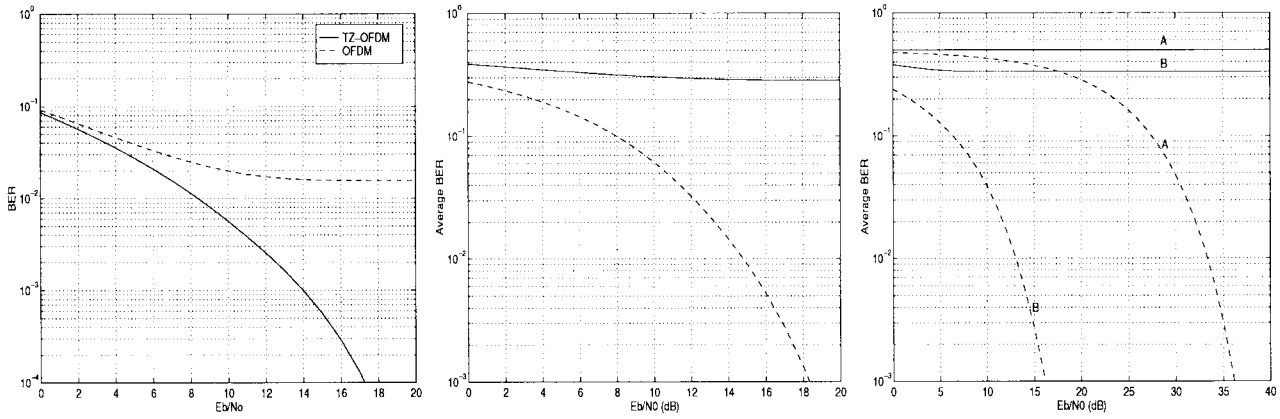

(a) (b) (c)

Fig. 5. (a) Average BER for OFDM (dashed) and TZ-OFDM/ZF (solid). (b) Average BER using Hadamard precoders with (dashed line) and without (solid line) scrambling. (c) Average BER using OFDM with cyclic prefix $(P, M, L, Q) = (8, 6, 4, 2)$, channel zeros $\exp(j2\pi l/P)$ (A), $\exp(j2\pi l/M)$ (B), $l = 0, \cdots, 3$, with (dashed line) and without (solid line) scrambling.

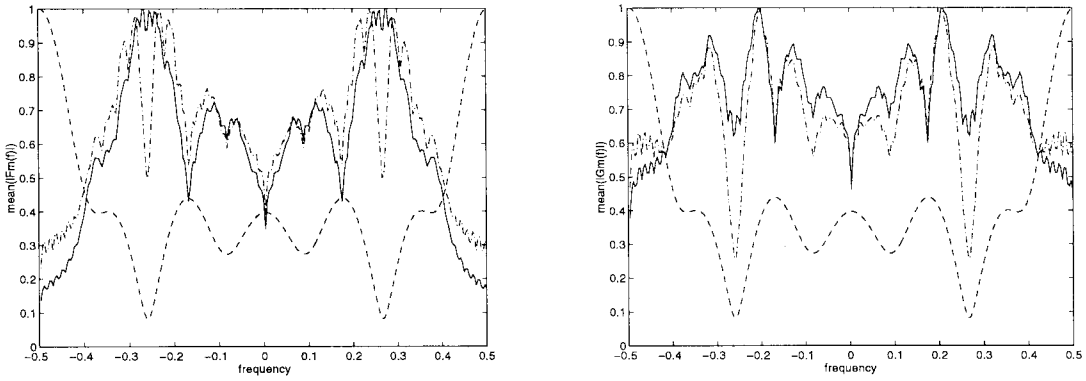

(a) (b)

Fig. 6. $|H(f)|$ (dashed) versus (a) average $|F_m(f)|$ (TZ solid, LZ dashed-dotted). Versus (b) average $|G_m(f)|$ (TZ solid, LZ dashed-dotted).

also statements 1.1a and 1.1c of Theorem 1 by testing the OFDM scheme without (solid line A) and with (dashed line A) scrambling. We used the same parameters as before, but with channel zeros at $\exp(j2\pi l/P)$, with $l = 0, \cdots, 3$. We observe that for both channels, use of aperiodic precoding achieves symbol recovery, whereas the schemes without scrambling do not allow symbol reconstruction, independent of the SNR.

Example 2—Optimum Max-SNR/ZF Designs: Here, we generate the optimal transmit/receive-filterbank pair of Theorem 3 with AWGN for the two cases of leading zeros (LZ) and trailing zeros (TZ) (57), with the proper definitions of the filterbank matrices provided in Section V-A. Our system parameters are $M = 32$, $P = 39$, $L = 7$, and the channel impulse response is $\boldsymbol{h}^T = [1, -0.3, 0.5, -0.4, 0.1, -0.02, 0.3, -0.1]$. Fig. 6(a) and (b) depict for both the LZ and TZ solutions the average magnitudes of the transmit- and receive-filters' transfer functions (each curve is normalized with respect to its maximum value)

$$|\mathcal{F}(f)| := \frac{1}{M}\sum_{m=1}^{M}|F_m(f)|$$

$$|\mathcal{G}(f)| := \frac{1}{M}\sum_{m=1}^{M}|G_m(f)|$$

together with the channel transfer function magnitude $|H(f)|$. Note that with both optimal designs, the transmit filterbank tends to pre-equalize the channel, i.e., to transmit more power at the frequencies where the channel attenuation is higher and vice-versa. Conversely, the frequency behavior of the receiver is more complicated to interpret because the receiver filterbank performs the equalization and, at the same time, produces white noise at its output.

Our method is also able to accommodate interferences superimposed to the received signal. In the following example, we consider two narrowband interferences superimposed to the receiver AWGN. Matrix $\boldsymbol{R}_{vv}$ was formed as the sum of the covariance matrices corresponding to the noise and the two interferences that are supposed to be uncorrelated with $v(n)$ and with interference-to-noise ratio $E_I/N_0 = E_s/N_0$. Using (56), we computed the optimal filterbanks for the TZ and LZ cases, whose frequency responses are reported in Fig. 7. We observe the deep nulls placed by the receive filterbanks on the frequencies occupied by the two interfering tones. Comparing the receive- with transmit-filterbank responses, we deduce that a considerable amount of power is wasted at the transmitter side at the frequencies occupied by the interferences.

To study the role of the TZ precoder and compare its performance with existing modulations, we computed the

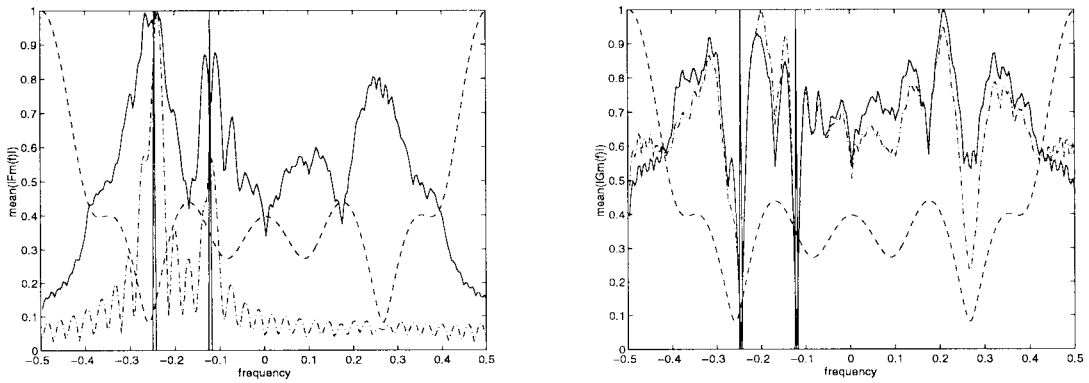

(a) (b)

Fig. 7. $|H(f)|$ (dashed) versus (a) average $|F_m(f)|$ (TZ solid, LZ dashed-dotted). (b) Versus average $|G_m(f)|$ (TZ solid, LZ dashed-dotted); interferences spectrum (solid).

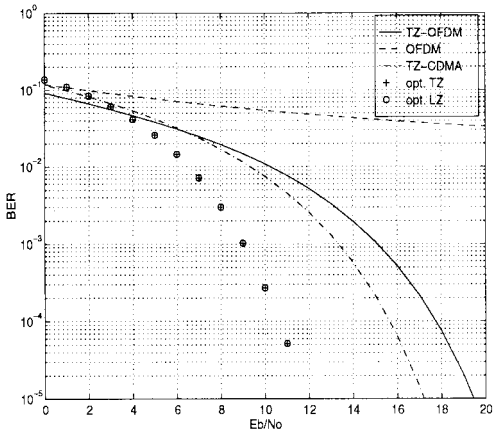

Fig. 8. BER versus E_b/N_0 (dB).

theoretical BER according to (78) and (79), assuming BPSK modulation with $M = 16$, $P = 20$, and $L = 4$ and using a channel with zeros at 1, $0.9j$, $-0.9j$, $1.3\exp(j\pi 5/8)$. The curves in Fig. 8 compare BER versus E_b/N_0 for the standard OFDM receiver [by inverting (15)], our proposed TZ-OFDM precoder and its receiver in (44), our optimized LZ-ZF and TZ-ZF transmitter-receiver pair in (57), and a TZ-CDMA precoder that uses as filters the Hadamard basis with trailing zeros and the corresponding receiver in (44). From Fig. 8, it is evident that the LZ-ZF and TZ-ZF optimal designs of (57) perform best and have basically identical BER. Standard OFDM exhibits the worst performance because it cannot equalize the subchannel located at zero frequency. It is also interesting that TZ-OFDM outperforms OFDM due to the null guard time used instead of the cyclic prefix (suffix). As illustrated by this example, the simple TZ modification is sufficient to meet the conditions of Theorem 1. Finally, using Hadamard codes instead of complex exponentials, most of the symbols are distributed across more than one frequency bin, and this makes TZ-CDMA more robust than TZ-OFDM, as verified by Fig. 8. This confirms that in general, spread spectrum codes are to be preferred in transmissions over frequency-selective channels.

Example 3—Optimum MMSE/CP Designs: Figs. 9 and 10 are the counterparts of Figs. 6 and 7 for the optimal transmitter-receiver filterbank pairs of Theorem 4 when the precoder has TZ's [see (74)] but for different levels of E_s/N_0. The same channel and parameters as in Figs. 6 and 7 were used, with $M = 32$, $P = 39$, and $L = 7$. It is interesting to provide an intuitive interpretation of the results shown in Fig. 9. In particular, the behavior of the transmit filters is strongly dependent on the values of E_s/N_0 at the receiver. More specifically, if E_s/N_0 is high, the transmitter tends to allocate more power at the most attenuated frequency bins; this is similar to the ZF case simulated in Example 2. In contrast, at low E_s/N_0, less power is concentrated at the most attenuated frequencies.

The difference in power allocation between the two optimization criteria is even more emphasized in the presence of narrowband interferences. As shown in Fig. 10(a), the MMSE-CP criterion does not waste as much power as the max-SNR/ZF criterion at the frequencies occupied by the interferences, especially at low E_s/N_0.

Example 4—Comparison of Optimal Designs: To compare the BER performance of the two design criteria under different channel selectivity conditions, we considered two channels: channel (a) with zeros at -1.1, $0.9j$, $0.7\exp(j3\pi/4)$ and channel (b) with zeros at 0.9, $0.7\exp(j2\pi 0.256)$, $0.4\exp(j2\pi 0.141)$. We generated BPSK symbols with $M = 8$ and $P = 11$ and computed both optimal TZ precoders according to (57) and (74). The resulting performance is reported in Fig. 11(a) and (b). We observe that both designs outperform OFDM, especially around the operational E_b/N_0 range of 10–20 dB. Comparing BER for the MMSE/CP and the max-SNR/ZF designs, it is worth noticing that in general, the MMSE-CP criterion yields lower BER at low E_b/N_0 values, where the noise predominates, whereas the max-SNR/ZF criterion provides better performance at high E_b/N_0 values, where the ISI constitutes the main source of error. Therefore, we expect that in general, the BER curves obtained with the two criteria intersect and the intersection point changes as a function of the channel selectivity, as evidenced in Fig. 11(a) and (b).

VII. Concluding Remarks

Redundancy in the input of digital communication systems is traditionally introduced in the form of error-correcting

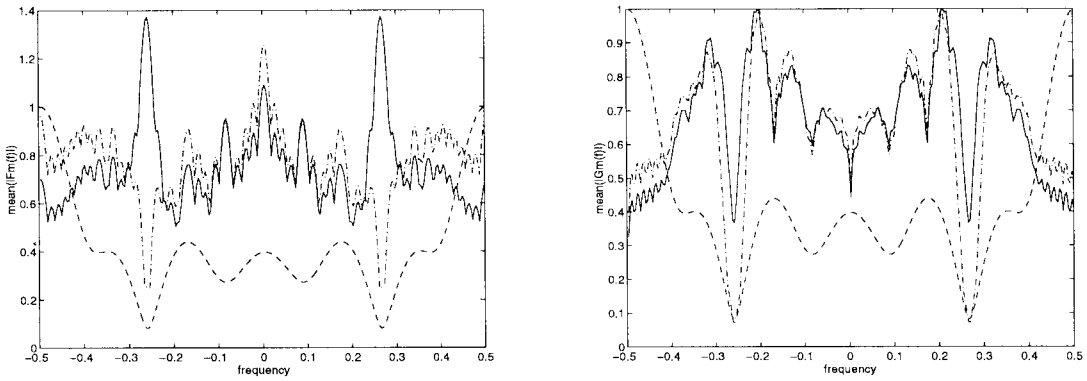

(a) (b)

Fig. 9. $|H(f)|$ (dashed) versus (a) average $|F_m(f)|$, $E_s/N_0 = 0$ dB (dashed-dotted), $E_s/N_0 = 20$ dB (solid). Versus (b) average $|G_m(f)|$, $E_s/N_0 = 0$ dB (dashed-dotted), $E_s/N_0 = 20$ dB (solid).

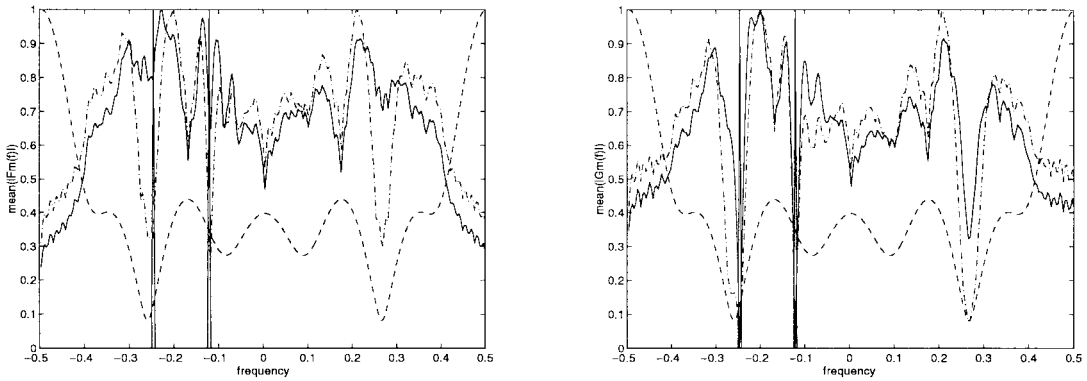

(a) (b)

Fig. 10. $|H(f)|$ (dashed) versus (a) average $|F_m(f)|$, $E_s/N_0 = 0$ dB (dashed-dotted), $E_s/N_0 = 20$ dB (solid). Versus (b) average $|G_m(f)|$, $E_s/N_0 = 0$ dB (dashed-dotted), $E_s/N_0 = 20$ dB (solid); interferences spectrum (solid).

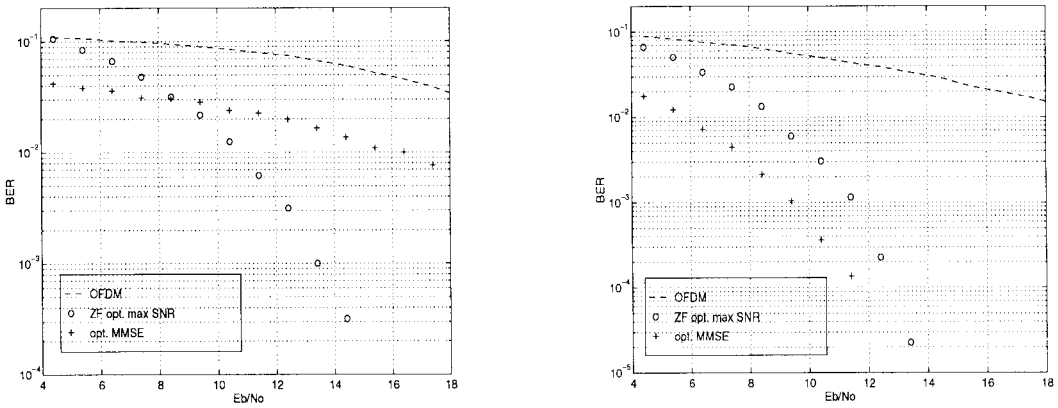

(a) (b)

Fig. 11. BER versus E_b/N_0 (dB) ($L = 3$, $M = 8$, $P = 11$).

codes defined over finite fields. In this paper, we developed redundant precoders in the form of FIR transmitter filterbanks and derived general existence and uniqueness conditions that guarantee perfect equalization of FIR channels with FIR receiver filterbanks. Contrary to existing approaches, no restrictions were imposed on the channel zero locations. Specific precoder designs with trailing zeros and receiver filterbanks with leading zeros were proved to yield simple and practical equalization algorithms for a number of single- and multiuser modulations that fall under the unifying FIR filterbank precoder-equalizer structure. With respect to OFDM precoders, the proposed transmit-receive filterbanks are more complex to obtain. However, this operation has to be done only once if the channel is time-invariant, or in case of time-varying channels, it needs to be performed every time the channel status information is updated. As far as real-time processing of the input data stream and of the equalizer input, with respect to OFDM, our approach requires more operations because it does not use the FFT; nevertheless, it relies on FIR filtering operations so that complexity does not increase dramatically.

However, the performance gained when dealing with practical channels that often exhibit deep nulls is worth the increased complexity.

Jointly optimal transmitter-receiver filterbanks were also designed to maximize output SNR with zero-forcing equalizers or minimize mean-square error with finite transmitted power constraints. The resulting designs turned out in closed form, and it is interesting to note that both design methodologies convert transmission over the wideband dispersive channel to transmission over P parallel uncorrelated subchannels, the main difference between the two approaches being the power distribution across the subchannels. For long distance transmissions where the transmitters have to operate at their maximum power, it is convenient to use the MMSE/CP criterion to avoid unnecessary waste of power on subchannels experiencing severe attenuation or narrowband interferences.

Although, in this paper, the channel was considered known and the reception was assumed to be block-synchronous, in a companion paper, we address blind symbol recovery and develop self-recovering equalization and synchronization algorithms [27]. Together with the results herein, *input diversity* induced by redundant filterbank precoders and scrambling turns out to be a very useful tool for mitigating multipath effects in block transmissions without requiring channel disparity conditions.

A number of interesting research issues open up: multichannel/multiuser extensions, adaptive algorithms, combined approaches that exploit input redundancy for joint error correction and channel equalization, and decision feedback alternatives along the lines of [36] and [37].

APPENDIX

Proof of (67): From (66), we can express $\boldsymbol{F}$ and $\boldsymbol{G}$ as

$$\boldsymbol{F}=\boldsymbol{V}\boldsymbol{\Phi}\boldsymbol{U}^H, \qquad \boldsymbol{G}=\boldsymbol{U}\boldsymbol{\Gamma}\boldsymbol{\Lambda}^{-1}\boldsymbol{V}^H\boldsymbol{H}^H\boldsymbol{R}_{vv}^{-1}. \tag{80}$$

In the TZ case, by substituting (80) to the terms in (59), we obtain

$$\begin{aligned}
&\mathrm{tr}(\boldsymbol{G}\boldsymbol{R}_{vv}\boldsymbol{G}^H)\\
&\quad=\mathrm{tr}(\boldsymbol{U}\boldsymbol{\Gamma}\boldsymbol{\Lambda}^{-1}\boldsymbol{V}^H\boldsymbol{H}^H\boldsymbol{R}_{vv}^{-1}\boldsymbol{R}_{vv}\boldsymbol{R}_{vv}^{-1}\boldsymbol{H}\boldsymbol{V}\boldsymbol{\Lambda}^{-1}\boldsymbol{\Gamma}^H\boldsymbol{U}^H)\\
&\quad=\mathrm{tr}(\boldsymbol{U}\boldsymbol{\Gamma}\boldsymbol{\Lambda}^{-1}\boldsymbol{V}^H\boldsymbol{V}\boldsymbol{\Lambda}\boldsymbol{V}^H\boldsymbol{V}\boldsymbol{\Lambda}^{-1}\boldsymbol{\Gamma}^H\boldsymbol{U}^H)\\
&\quad=\mathrm{tr}(\boldsymbol{\Gamma}\boldsymbol{\Lambda}^{-1}\boldsymbol{\Gamma}^H)\\
&\mathrm{tr}((\boldsymbol{G}\boldsymbol{H}\boldsymbol{F}-\boldsymbol{I})\boldsymbol{R}_{ss}(\boldsymbol{G}\boldsymbol{H}\boldsymbol{F}-\boldsymbol{I})^H)\\
&\quad=\mathrm{tr}((\boldsymbol{U}\boldsymbol{\Gamma}\boldsymbol{\Lambda}^{-1}\boldsymbol{\Lambda}\boldsymbol{\Phi}\boldsymbol{U}^H-\boldsymbol{I})\boldsymbol{R}_{ss}(\boldsymbol{U}\boldsymbol{\Gamma}\boldsymbol{\Lambda}^{-1}\boldsymbol{\Lambda}\boldsymbol{\Phi}\boldsymbol{U}-\boldsymbol{I})^H)\\
&\quad=\mathrm{tr}(\boldsymbol{U}(\boldsymbol{\Gamma}\boldsymbol{\Phi}-\boldsymbol{I})\boldsymbol{U}^H\boldsymbol{R}_{ss}\boldsymbol{U}(\boldsymbol{\Gamma}\boldsymbol{\Phi}-\boldsymbol{I})^H\boldsymbol{U}^H)\\
&\quad=\mathrm{tr}((\boldsymbol{\Gamma}\boldsymbol{\Phi}-\boldsymbol{I})\boldsymbol{\Delta}(\boldsymbol{\Gamma}\boldsymbol{\Phi}-\boldsymbol{I})^H)\\
&\mathrm{tr}(\boldsymbol{F}\boldsymbol{R}_{ss}\boldsymbol{F}^H)\\
&\quad=\mathrm{tr}(\boldsymbol{V}\boldsymbol{\Phi}\boldsymbol{U}^H\boldsymbol{U}\boldsymbol{\Delta}\boldsymbol{U}^H\boldsymbol{U}\boldsymbol{\Phi}^H\boldsymbol{V}^H)\\
&\quad=\mathrm{tr}(\boldsymbol{\Phi}\boldsymbol{\Delta}\boldsymbol{\Phi}^H).
\end{aligned}\tag{81}$$

Thus, (59) can be written as

$$\begin{aligned}
\mathcal{E}+\mu\mathcal{C}=&\,\mathrm{tr}(\boldsymbol{\Gamma}\boldsymbol{\Lambda}^{-1}\boldsymbol{\Gamma}^H)+\mathrm{tr}((\boldsymbol{\Gamma}\boldsymbol{\Phi}-\boldsymbol{I})\boldsymbol{\Delta}(\boldsymbol{\Gamma}\boldsymbol{\Phi}-\boldsymbol{I})^H)\\
&+\mu(\mathrm{tr}(\boldsymbol{\Phi}\boldsymbol{\Delta}\boldsymbol{\Phi}^H)-P_0).
\end{aligned}\tag{82}$$

In the LZ case, using the appropriate decomposition of $\boldsymbol{H}^H\boldsymbol{R}_{vv}^{-1}\boldsymbol{H}$ specified in (55), we obtain the same result, considering that

$$\begin{aligned}
&\boldsymbol{V}^H(\boldsymbol{V},\boldsymbol{V}_n)\begin{pmatrix}\boldsymbol{\Lambda}&\boldsymbol{0}\\ \boldsymbol{0}&\boldsymbol{0}\end{pmatrix}(\boldsymbol{V},\boldsymbol{V}_n)^H\boldsymbol{V}\\
&\quad=(\boldsymbol{I},\boldsymbol{0})\begin{pmatrix}\boldsymbol{\Lambda}&\boldsymbol{0}\\ \boldsymbol{0}&\boldsymbol{0}\end{pmatrix}(\boldsymbol{I},\boldsymbol{0})^H=\boldsymbol{\Lambda}.
\end{aligned}\tag{83}$$

■

Proof of Lemma:

Proof: From (68) and (69), we can obtain, respectively

$$\boldsymbol{\Gamma}^H\boldsymbol{\Gamma}\boldsymbol{\Phi}\boldsymbol{\Delta}\boldsymbol{\Phi}^H+\boldsymbol{\Gamma}^H\boldsymbol{\Gamma}\boldsymbol{\Lambda}^{-1}=\boldsymbol{\Gamma}^H\boldsymbol{\Delta}\boldsymbol{\Phi}^H \tag{84}$$

$$\mu\boldsymbol{\Phi}\boldsymbol{\Delta}\boldsymbol{\Phi}^H+\boldsymbol{\Gamma}^H\boldsymbol{\Gamma}\boldsymbol{\Phi}\boldsymbol{\Delta}\boldsymbol{\Phi}^H=\boldsymbol{\Gamma}^H\boldsymbol{\Delta}\boldsymbol{\Phi} \tag{85}$$

and after equating the left-hand sides of (84) and (85), we get

$$\mu\boldsymbol{\Phi}\boldsymbol{\Delta}\boldsymbol{\Phi}^H=\boldsymbol{\Gamma}^H\boldsymbol{\Gamma}\boldsymbol{\Lambda}^{-1}. \tag{86}$$

Because matrix $\mu\boldsymbol{\Phi}\boldsymbol{\Delta}\boldsymbol{\Phi}^H$ is Hermitian, $\boldsymbol{\Gamma}^H\boldsymbol{\Gamma}\boldsymbol{\Lambda}^{-1}$ must be Hermitian too, and thus, $\boldsymbol{\Gamma}^H\boldsymbol{\Gamma}\boldsymbol{\Lambda}^{-1}=\boldsymbol{\Lambda}^{-1}\boldsymbol{\Gamma}^H\boldsymbol{\Gamma}$. For distinct[7] λ_{ii}'s the latter is possible only if $\boldsymbol{\Gamma}^H\boldsymbol{\Gamma}$ is diagonal. Hence, $\boldsymbol{\Gamma}^H\boldsymbol{\Gamma}$ is diagonal and, due to (86), $\boldsymbol{\Phi}\boldsymbol{\Delta}\boldsymbol{\Phi}^H$ must be diagonal as well.

To show that $\mu\boldsymbol{\Phi}\boldsymbol{\Delta}^2\boldsymbol{\Phi}^H$ is also diagonal, we use again (68) and (69) to obtain

$$\boldsymbol{\Phi}\boldsymbol{\Delta}\boldsymbol{\Phi}^H(\boldsymbol{\Gamma}^H\boldsymbol{\Gamma}+\mu\boldsymbol{I})(\boldsymbol{\Lambda}^{-1}+\boldsymbol{\Phi}\boldsymbol{\Delta}\boldsymbol{\Phi}^H)=\boldsymbol{\Phi}\boldsymbol{\Delta}^2\boldsymbol{\Phi}^H. \tag{87}$$

Because $\boldsymbol{\Phi}\boldsymbol{\Delta}\boldsymbol{\Phi}^H$ and $\boldsymbol{\Gamma}^H\boldsymbol{\Gamma}$ are diagonal, the right-hand side of (87) must be also diagonal. ■

Proof of (70): Substituting (68) into the MSE part of (67), we obtain

$$\begin{aligned}
\mathcal{E}&=\mathrm{tr}(\boldsymbol{\Delta}-\boldsymbol{\Delta}\boldsymbol{\Phi}^H(\boldsymbol{\Lambda}^{-1}+\boldsymbol{\Phi}\boldsymbol{\Delta}\boldsymbol{\Phi}^H)^{-1}\boldsymbol{\Phi}\boldsymbol{\Delta})\\
&=\mathrm{tr}(\boldsymbol{\Delta}-(\boldsymbol{\Lambda}^{-1}+\boldsymbol{\Phi}\boldsymbol{\Delta}\boldsymbol{\Phi}^H)^{-1}\boldsymbol{\Phi}\boldsymbol{\Delta}^2\boldsymbol{\Phi}^H).
\end{aligned}\tag{88}$$

Due to the Lemma, the matrix inside the trace is diagonal and can be written explicitly as

$$\mathcal{E}=\sum_i\left(\delta_{ii}-\frac{\sum_j|\phi_{ij}|^2\delta_{jj}^2}{\lambda_{ii}^{-1}+\sum_j|\phi_{ij}|^2\delta_{jj}}\right). \tag{89}$$

As far as minimizing $\mathcal{E}+\mu\mathcal{C}$, we will argue that w.l.o.g. matrix $\boldsymbol{\Phi}$ can have at most one nonzero entry in every row and every column; furthermore, we will show next that matrix $\boldsymbol{\Phi}$ can be considered w.l.o.g. as diagonal.

For each row i, let $\delta_{JJ}:=\max_j\delta_{jj}$, and define $\hat{\boldsymbol{\Phi}}$ such that

$$\delta_{JJ}|\hat{\phi}_{iJ}|^2=\sum_j|\phi_{ij}|^2\delta_{jj} \quad\text{and}\quad \hat{\phi}_{ij}=0 \qquad \text{if } j\neq J. \tag{90}$$

Due to (90), we have $\mathrm{tr}(\boldsymbol{\Phi}\boldsymbol{\Delta}\boldsymbol{\Phi}^H)=\mathrm{tr}(\hat{\boldsymbol{\Phi}}\boldsymbol{\Delta}\hat{\boldsymbol{\Phi}}^H)$, i.e., if $\boldsymbol{\Phi}$ satisfies the power constraint, then so does $\hat{\boldsymbol{\Phi}}$. Moreover,

[7] When $\boldsymbol{\Lambda}$ has repeated eigenvalues, define $\boldsymbol{\Lambda}=\boldsymbol{\Lambda}+\delta\boldsymbol{\Lambda}$ with $\delta\boldsymbol{\Lambda}$ a diagonal perturbation matrix to assure that λ_{ii}'s are distinct. However, $\phi_{ii}(\boldsymbol{\Lambda})$ in (73) is a continuous function of $\boldsymbol{\Lambda}$, which implies that $\lim_{\delta\boldsymbol{\Lambda}\to\boldsymbol{0}}\phi_{ii}(\boldsymbol{\Lambda})=\phi_{ii}(\boldsymbol{\Lambda})$ and proves that Theorem 4 holds true as well for channels with repeated eigenvalues.

because $\sum_j |\phi_{ij}|^2\delta_{jj}^2 > 0$, using the definition of δ_{JJ}, we find

$$\sum_j |\phi_{ij}|^2\delta_{jj}^2 \le \delta_{JJ}\sum_j |\phi_{ij}|^2\delta_{jj} = |\hat{\phi}_{iJ}|^2\delta_{JJ}^2. \qquad (91)$$

From (91) and (89), we infer that if $\mathbf{\Phi}$ minimizes $\mathcal{E}$, then so does $\hat{\mathbf{\Phi}}$. Hence, as far as minimizing $\mathcal{E}+\mu\mathcal{C}$, we can take $\mathbf{\Phi} = \hat{\mathbf{\Phi}}$ to have only one nonzero entry per row. Since $\mathbf{\Phi}$ must be full rank, it should also have only one nonzero entry per column; thus $\mathbf{\Phi}$ should be (within a permutation matrix factor) diagonal, but permutation matrices do not alter $\mathcal{C}\mathbf{\Phi}$; hence, setting λ_{ii}'s and δ_{ii}'s in decreasing order, forces w.l.o.g. $\mathbf{\Phi}$ to be diagonal [c.f. (90)]. ■

REFERENCES

[1] A. N. Akansu, P. Duhamel, X. Lin, and M. de Courville "Orthogonal transmultiplexers in communication: A review," *IEEE Trans. Signal Processing*, vol. 46, pp. 979–995, Apr. 1998.

[2] S. Benedetto, E. Biglieri, and V. Castellani, *Digital Transmission Theory*. Englewood Cliffs, NJ: Prentice-Hall, 1987.

[3] J. S. Chow, J. C. Tu, and J. M. Cioffi, "A discrete multitone transceiver system for HDSL applications," *IEEE J. Select. Areas Commun.*, vol. 9, pp. 895–908, Aug. 1991.

[4] A. Chevreuil and P. Loubaton, "Blind second-order identification of FIR channels: Forced cyclostationarity and structured subspace method," *IEEE Signal Processing Lett.*, vol. 4, pp. 204–206, July 1997.

[5] L. J. Cimini, "Analysis and simulation of a digital mobile channel using orthogonal frequency division multiple access," *IEEE Trans. Commun.*, vol. 42, pp. 665–675, 1995.

[6] M. de Courville, P. Duhamel, P. Madec, and J. Palicot, "A least mean-squares blind equalization technique for OFDM systems," *Ann. Télécommun.*, pp. 4–11, 1997.

[7] Z. Ding, "Characteristics of band-limited channels unidentifiable from second-order cyclostationary statistics," *IEEE Signal Processing Lett.*, vol. 3, pp. 150–152, May 1996.

[8] Euro. Telecommun. Stand., "Radio broadcast systems: Digital audio broadcasting (DAB) to mobile, portable, and fixed receivers," preETS 300 401, Mar. 1994.

[9] A. Delopoulos and S. P. Kollias, "Optimal filter banks for perfect reconstruction from noisy subband components," *IEEE Trans. Signal Processing*, vol. 44, pp. 212–224, Feb. 1996.

[10] N. J. Fliege, "Orthogonal multiple carrier data transmission," *Euro. Trans. Telecommun.*, vol. 3, no. 3, pp. 255–264, May 1992.

[11] G. D. Forney, Jr. and M. V. Eyuboğlu, "Combined equalization and coding using precoding," *IEEE Commun. Mag.*, pp. 25–34, Dec. 1991.

[12] D. A. George, "Matched filters for interfering signals," *IEEE Trans. Inform. Theory*, pp. 153–154, 1965.

[13] G. B. Giannakis, "Filterbanks for blind channel identification and equalization," *IEEE Signal Processing Lett.*, vol. 4, pp. 184–187, June 1997.

[14] ———, "Cyclostationary signal analysis," in *Digital Signal Processing Handbook*, V. K. Madisetti and D. Williams, Eds. Boca Raton, FL: CRC, 1998.

[15] G. B. Giannakis and S. Halford, "Blind fractionally-spaced equalization of noisy FIR channels: Direct and adaptive solutions," *IEEE Trans. Signal Processing*, vol. 45, pp. 2277–2292, Sept. 1997.

[16] G. H. Golub and C. F. Van Loan, *Matrix Computations*. Baltimore, MD: Johns Hopkins Univ. Press, 1991, sec. 5.5.4.

[17] K. Gosse and P. Duhamel, "Perfect reconstruction versus MMSE filterbanks in source coding," *IEEE Trans. Signal Processing*, vol. 45, pp. 2188–2202, Sept. 1997.

[18] S. D. Halford and G. B. Giannakis, "Blind equalization of TDMA wireless channels exploiting guard time induced cyclostationarity," in *Proc. 1st IEEE Signal Process. Workshop Wireless Commun.*, Paris, France, Apr. 16–18, 1997, pp. 117–120.

[19] I. Kalet, "The multitone channel," *IEEE Trans. Commun.*, vol. 37, pp. 119–124, Feb. 1989.

[20] J. W. Lechleider, "The optimum combination of block codes and receivers for arbitrary channels," *IEEE Trans. Commun.*, vol. 38, pp. 615–621, May 1990.

[21] L. Lupas, "On the computation of generalized Vandermonde matrix inverse," *IEEE Trans. Automat. Contr.*, vol. AC-20, pp. 559–561, 1975.

[22] E. Moulines, P. Duhamel, J. Cardoso, and S. Mayrargue, "Subspace methods for the blind identification of multichannel FIR filters," *IEEE Trans. Signal Processing*, vol. 43, pp. 516–525, Feb. 1995.

[23] E. Nikula, A. Toskala, E. Dahlman, L. Girard, and A. Klein, "FRAMES multiple access for UMTS and IMT-2000," *IEEE Trans. Prof. Commun.*, vol. 41, pp. 216–224, Apr. 1998.

[24] J. G. Proakis, *Digital Communication.* New York: McGraw-Hill, 1995.

[25] A. Ruiz, J.M. Cioffi, and S. Kasturia, "Discrete multiple tone modulation with coset coding for the spectrally shaped channel," *IEEE Trans. Commun.*, vol. 40, pp. 1012–1029, June 1992.

[26] S. D. Sandberg and M. A. Tzannes, "Overlapped discrete multitone modulation for high speed copper wire communications," *IEEE J. Select. Areas Commun.*, vol. 13, pp. 1571–1585, Dec. 1995.

[27] A. Scaglione, G. B. Giannakis, and S. Barbarossa, "Redundant filterbank precoders and equalizers Part II: Blind signal recovery," *IEEE Trans. Signal Processing*, this issue, pp. 2007–2022; see also *Proc. 35th Allerton Conf. Commun., Contr., Comput.*, Sept. 1997, pp. 385–394; *Proc. Int. Conf. Acoust., Speech, Signal Process.*, Seattle, WA, May 12–15, 1998, vol. VI, pp. 3501–3504.

[28] A. Scaglione, S. Barbarossa, and G. B. Giannakis "Filterbank transceivers optimizing information rate in block transmissions over dispersive channels," *IEEE Trans. Inform. Theory*, vol. 45, pp. 1019–1032, Apr. 1999.

[29] E. Serpedin and G. B. Giannakis, "Blind channel identification and equalization with modulation induced cyclostationarity," *IEEE Trans. Signal Processing*, vol. 46, pp. 1930–1944, July 1998.

[30] M. K. Tsatsanis and G. B. Giannakis, "Optimal linear receivers for DS-CDMA systems: A signal processing approach," *IEEE Trans. Signal Processing*, vol. 44, pp. 3044–3055, Dec. 1996.

[31] ———, "Blind estimation of direct sequence spread spectrum signals in multipath," *IEEE Trans. Signal Processing*, vol. 45, pp. 1241–1252, May 1997.

[32] ———, "Transmitter induced cyclostationarity for blind channel equalization," *IEEE Trans. Signal Processing*, vol. 45, pp. 1785–1794, July 1997.

[33] L. Tong, G. Xu, and T. Kailath, "Blind identification and equalization based on second order statistics: A time domain approach," *IEEE Trans. Inform. Theory*, vol. 40, pp. 340–349, Mar. 1994.

[34] L. Tong, G. Xu, B. Hassibi, and T. Kailath, "Blind channel identification based on second-order statistics: A frequency-domain approach," *IEEE Trans. Inform. Theory*, vol. 41, pp. 329–334, Jan. 1995.

[35] P. P. Vaidyanathan, *Multirate Systems and Filter Banks.* Englewood Cliffs, NJ: Prentice-Hall, 1993.

[36] L. Vandendorpe, "MMSE equalizers for multitone systems without guard time," in *Proc. 8th Euro. Signal Process. Conf.*, Trieste, Italy, Sept. 1996.

[37] L. Vandendorpe, L. Cuvelier, F. Deryck, J. Louveaux, and O. van de Wiel, "Fractionally spaced linear and decision-feedback detectors for transmultiplexers," *IEEE Trans. Signal Processing*, vol. 46, pp. 996–1011, Apr. 1998.

[38] G. Wornell, "Emerging applications of multirate signal processing and wavelets in digital communications," *Proc. IEEE*, vol. 84, pp. 586–603, Apr. 1996.

[39] X.-G. Xia, "New precoding for intersymbol interference cancellation using nonmaximally decimated multirate filterbanks with ideal FIR equalizers," *IEEE Trans. Signal Processing*, vol. 45, pp. 2431–2440, Oct. 1997.

[40] J. Yang and S. Roy, "On joint transmitter and receiver optimization for multiple-input–multiple-output (MIMO) transmission systems," *IEEE Trans. Commun.*, vol. 42, pp. 3221–3231, Dec. 1994.

[41] W. Y. Zou and Y. Wu, "COFDM: An overview," *IEEE Trans. Broadcasting*, vol. 41, pp. 1–8, Mar. 1995.

Anna Scaglione (S'97) received the B.S. and Ph.D. degrees in electrical engineering from the the Information and Communication Department, University of Rome "La Sapienza," Rome, Italy, in 1995 and 1999, respectively.

In 1997, she visited the University of Virginia, Charlottesville, as a Research Assistant, and since March 1999, she has been with the Electrical and Computer Engineering Department, University of Minnesota, Minneapolis, as a Postdoctoral Researcher. Her general interests lie in the area of statistical signal processing and multirate filterbanks. Specific research areas of current interest include polynomial-phase signal modeling for SAR applications and demodulation of CPM signals, multirate filterbanks for CDMA, and equalization over frequency selective channels.

Georgios B. Giannakis (F'96) received the Diploma in electrical engineering from the National Technical University of Athens, Athens, Greece in 1981. From September 1982 to July 1986, he was with the University of Southern California (USC), where he received the M.Sc. degree in electrical engineering in 1983, the M.Sc. degree in mathematics in 1986, and the Ph.D. degree in electrical engineering in 1986.

After lecturing for one year at USC, he joined the University of Virginia (UVA), Charlottesville, in 1987, where he became a Professor of Electrical Engineering in 1997, Graduate Committee Chair, and Director of the Communications, Controls, and Signal Processing Laboratory in 1998. Since January 1999, he has been with the University of Minnesota, Minneapolis, as a Professor of Electrical and Computer Engineering. His general interests lie in the areas of signal processing and communications, estimation and detection theory, time-series analysis, and system identification—subjects on which he has published more than 90 journal papers. Specific areas of expertise include (poly)spectral analysis, wavelets, cyclostationary, and non-Gaussian signal processing with applications to SAR, array, and image processing. Current research topics focus on transmitter and receiver diversity techniques for equalization of single- and multiuser communication channels, mitigation of fading, compensation of nonlinear effects, redundant filterbank transceivers for block transmissions, multicarrier, and wideband communication systems.

Dr. Giannakis received the IEEE Signal Processing Society's 1992 Paper Award in the Statistical Signal and Array Processing (SSAP) area. He also co-authored the winner of the IEEE-SP 1998 Best Paper Award (under 30-year old category). During his 12 years at UVA, he was awarded the School of Engineering and Applied Science Junior Faculty Research Award in 1988, and the EE Outstanding Faculty Teaching Award in 1992. He co-organized the 1993 IEEE Signal Processing Workshop on Higher Order Statistics, the 1996 IEEE Workshop on Statistical Signal and Array Processing, and the first IEEE Signal Processing Workshop on Wireless Communications in 1997. He guest (co-)edited two Special Issues on High-Order Statistics (*International Journal of Adaptive Control and Signal Processing* and the EURASIP journal *Signal Processing*) and the January 1997 Special Issue on Signal Processing for Advanced Communications of the IEEE TRANSACTIONS ON SIGNAL PROCESSING. He has served as an Associate Editor for the IEEE TRANSACTIONS ON SIGNAL PROCESSING and the IEEE SIGNAL PROCESSING LETTERS, a secretary of the Signal Processing Conference Board, a member of the SP Publications Board, and a Member and Vice-Chair of the SSAP Technical Committee. He now chairs the Signal Processing for Communications Technical Committee. He is also a member of the IMS and the European Association for Signal Processing.

Sergio Barbarossa (M'88) received the M.Sc. and Ph.D. degrees in electrical engineering from the University of Rome "La Sapienza," Rome, Italy, in 1984 and 1988, respectively.

From 1984 to 1986, he worked with Selenia as a Radar System Engineer. Since 1986, he has been with the Information and Communication Department, University of Rome "La Sapienza," where he is an Associate Professor. In 1988, on leave from the University of Rome, he was a Research Engineer at the Environmental Research Institute of Michigan, Ann Arbor. During the spring of 1995 and the summer of 1997, he was a Visiting Faculty Member with the Department of Electrical Engineering, University of Virginia, Charlottesville. His general interests are in the area of statistical signal processing with applications to radar and communications.

Dr. Barbarossa is a Member of the IEEE Technical Committee on Signal Processing for Communications and is currently serving as an Associate Editor for the IEEE TRANSACTIONS ON SIGNAL PROCESSING.